

การใช้เทคนิคเอทีอาร์เอฟทีไออาร์สเปกโทรสโกปีเพื่อหาความหนาแน่นของการเชื่อมขวาง
ของฟิล์มโคโตนที่ความลึกต่างๆ



นาย วุฒิพงษ์ พึ่งพิพัฒนา

สถาบันวิทยบริการ จุฬาลงกรณ์มหาวิทยาลัย

วิทยานิพนธ์นี้เป็นส่วนหนึ่งของการศึกษาตามหลักสูตรปริญญาวิทยาศาสตรมหาบัณฑิต
สาขาวิชาวิทยาศาสตร์พอลิเมอร์ประยุกต์และเทคโนโลยีสิ่งทอ ภาควิชาวัสดุศาสตร์

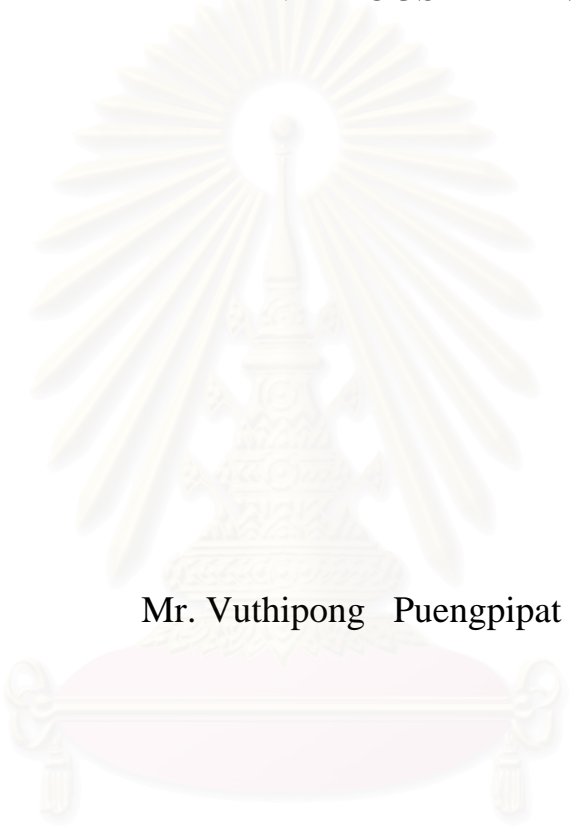
คณะวิทยาศาสตร์ จุฬาลงกรณ์มหาวิทยาลัย

ปีการศึกษา 2544

ISBN 974-03-0479-6

ลิขสิทธิ์ของจุฬาลงกรณ์มหาวิทยาลัย

USE OF ATR FT-IR SPECTROSCOPY TECHNIQUE TO
DETERMINE THE CROSSLINKING DENSITY OF CHITOSAN
FILM AT VARIOUS DEPTHS



Mr. Vuthipong Puengpipat

สถาบันวิทยบริการ
จุฬาลงกรณ์มหาวิทยาลัย

A Thesis Submitted in Partial Fulfillment of the Requirements
for the Degree of Master of Science in Applied Polymer Science and Textile Technology
Department of Materials Science
Faculty of Science
Chulalongkorn University
Academic Year 2001
ISBN 974-03-0479-6

Thesis Title Use of ATR FT-IR Spectroscopy Technique to Determine the
 Crosslinking Density of Chitosan Film at Various Depths
By Mr. Vuthipong Puengpipat
Department Materials Science
Thesis Advisor Associated. Professor. Khemchai Hemachandra, Ph.D.
Thesis Co-advisor Assistant. Professor. Sanong Ekgasit, Ph.D.

Accepted by Faculty of Science, Chulalongkorn University in Partial
Fulfillment of the Requirements for the Master's Degree.

.....Dean of Faculty of Science
(Associate Professor Wanchai Phothiphichitr, Ph.D.)

Thesis Committee

.....Chairman
(Associate Professor Saowaroj Chuayjuljit)

.....Thesis Advisor
(Associate Professor Khemchai Hemachandra, Ph.D.)

.....Thesis Co-advisor
(Assistant Professor Sanong Ekgasit, Ph.D.)

.....Member
(Associate Professor Werasak Udomkichdecha, Ph.D.)

.....Member
(Associate Professor Paiparn Santisuk)

4172451423 : MAJOR APPLIED POLYMER SCIENCE AND TEXTILE TECHNOLOGY

KEY WORD: ATR FT-IR, INFRARED SPECTROSCOPY, DEPTH PROFILING, CROSSLINKING DENSITY, CHITOSAN, GLUTARALDEHYDE
 VUTHIPONG PUENGPIPAT: USE OF ATR FT-IR SPECTROSCOPY TECHNIQUE TO DETERMINE THE CROSSLINKING DENSITY OF CHITOSAN FILM AT VARIOUS DEPTHS. THESIS ADVISOR: ASSOC. PROF. KHEMCHAI HEMACHANDRA, Ph.D. THESIS CO-ADVISOR: ASST. PROF. SANONG EKGASIT, Ph.D. 90 pp. ISBN 974-03-0479-6.

Crosslinking density of chitosan films plays an important role in the properties of chitosan films. However, there are only small numbers of researches, which determine the crosslinking density at various depths. The objective of this research is to determine the crosslinking density at various depths of chitosan films crosslinked with glutaraldehyde by heterogeneous procedure. The technique used to determine the crosslinking density was attenuated total reflection Fourier transform infrared (ATR FT-IR) spectroscopy. By varying the angles of incidence and performing mathematical operation on the observed spectra, the information at various depths of the films in terms of nk values were achieved. The results showed that the crosslinking density was not uniform over the entire thickness of the film. The crosslinking density was highest at the surface, which contacted directly with crosslinking solution and decreased as a function of depth. Moreover, it was found that crosslinking reaction was occurred at the 10 μm depths from crosslinked surface.

Department of Materials Science
 Field of study Applied Polymer Science and Textile Technology
 Academic Year 2001

Student's Signature.....
 Advisor's Signature.....
 Co-advisor's Signature.....

ACKNOWLEDGEMENTS

I wish to express my deep gratitude to my thesis co-advisor and advisor, Asst. Prof. Dr. Sanong Ekgasit and Assoc. Prof. Dr. Khemchai Hemachandra, who always provide me the useful guidance, suggestion, encouragement, and understanding and also patiently practise my technical skill during the whole research.

Gratefully thanks to Assoc. Prof. Saowaroj Chuayjuljit, Assoc. Prof. Dr. Weerasak Udomkichdecha, and Assoc. Prof. Paiparn Santisuk for their substantial advice as thesis committee.

I also would like to acknowledge computer and other academic facility supply from the Spectroscopy Group at the Department of Chemistry for computer assisted chemical education and research and instrumental support from Bruker Analytical and Medical Instrument South East Asia.

I gratefully acknowledge the financial support from the National Science and Technology Development Agency, Ministry of Science and Technology and Energy via Local Graduate Scholarship.

My thanks are also extended to the Metallurgy and Materials Science Research Institute and the staff especially to Mrs. Krisana Siraleartmukul and Mrs. Sarintorn Limpanath for their kind assistance.

Thanks to all my friends especially Miss Adchara Padermshoke, Miss Daranee Tonketmongkon, Mr. Weeradej Silpsamrith, Miss Siriluk Chiarakorn, Mr. Korndanai Akawat, and Mr. Viwat Vchirawongkwin for their kindly help.

Finally, I would like to affectionately give all gratitude to the members of my family for their wholehearted understanding, encouragement, and patient support throughout my entire study.

CONTENTS

	Pages
ABSTRACT IN THAI.....	iv
ABSTRACT IN ENGLISH.....	v
ACKNOWLEDGEMENTS.....	vi
LIST OF FIGURES.....	xi
LIST OF TABLES.....	xv
LIST OF ABBREVIATIONS.....	xvi
LIST OF SYMBOLS.....	xvi
CHAPTER 1 INTRODUCTION.....	1
CHAPTER 2 THEORETICAL BACKGROUND.....	3
2.1. Chitosan	3
2.1.1. Introduction.....	3
2.1.2. Chitin Manufacturing Process.....	4
2.1.3. Chitosan Manufacturing Process.....	8
2.1.4. Characteristics of Chitosan.....	8
2.1.5. Applications.....	12
2.2. Crosslinking of Chitosan.....	14
2.2.1. Background.....	14
2.2.2. Crosslinking Reaction of Chitosan.....	15
2.2.2.1. Crosslinking Reaction with Glutaraldehyde	15
2.2.2.2. Crosslinking Procedure of Chitosan with	
Glutaraldehyde.....	17
2.3. Infrared Spectroscopy.....	22
2.3.1. Basic Concepts of Spectroscopy.....	22
2.3.2. Reflection and Refraction.....	24

	Pages
CHAPTER 4 RESULTS AND DISCUSSION.....	44
4.1. Preparation of Crosslinked Chitosan Films.....	44
4.2. Accuracy of Programs Used for <i>nk</i> value Calculation.....	46
4.3. <i>nk</i> Value of Isotropic Substrate.....	50
4.4. <i>nk</i> Value of Chitosan Film.....	52
4.5. <i>nk</i> Value of Crosslinked Chitosan Films.....	56
CHAPTER 5 CONCLUSION.....	69
REFERENCES.....	70
APPENDICES.....	76
VITAE	90

สถาบันวิทยบริการ
จุฬาลงกรณ์มหาวิทยาลัย

LIST OF FIGURES

	Pages
2.1 Structures of Cellulose, Chitin, and Chitosan.....	4
2.2 Crosslinking Reaction Between Chitosan and Glutaraldehyde.....	15
2.3 Proposed Structure for Chitosan Crosslinked by Glutaraldehyde.....	16
2.4 Infrared Spectra Glutaraldehyde, Chitosan and Crosslinked Chitosan...	17
2.5 Propagation of a Linearly Polarized Electromagnetic Wave in the Direction of Propagation.....	22
2.6 Interactions of Light With Matter.....	23
2.7 Reflection and Refraction at the Interface of two Media with Different Refractive Index. in This Case $n_1 < n_2$ Snell's Law.....	25
2.8 Reflection and Refraction at Critical Angle.....	25
2.9 Selected IRE Configurations Commonly Used in ATR Experimental Setups: a.) Single Reflection Variable-Angle Hemispherical or Hemicylinder Crystal, and b.) Multiple Reflection Single-pass Crystal.....	27
2.10 The Seagull™ Variable Angle Reflection Attachment.....	28
2.11 Relationship Between MSEF and Depth at Various Experimental Conditions (A, A') and Its Decay Characteristic (B, B'). The Simulation Parameters are $n_0 = 4.0$ for Ge IRE, $n_0 = 2.40$ for ZnSe IRE, $\nu = 1,000 \text{ cm}^{-1}$, $n_1(\nu) = 1.5$, and $k_1(\nu) = 0.0, 0.1, 0.2, 0.3, 0.4, \text{ and } 0.5 \dots$	32
2.12 Penetration Depth at Various Experimental Conditions for Germanium and Zinc Selenide IRE.....	34
4.1 Transmission Spectra of Chitosan Films Crosslinked With Various Crosslinking Times.....	45
4.2 Simulated ATR Spectra of Film at Various Angles of Incidence. The Simulation Parameters are $n_{\text{film}}=1.4$, $n_{\text{IRE}}=4.0$, $k_{\text{film}}=0.02$, Angles of Incidence=37, 39, 41, 43, 45, 47, and 49 Degree.....	48
4.3 Simulated ATR Spectra of Film at Various Angles of Incidence. The Simulation Parameters are $n_{\text{film}}=1.4$, $n_{\text{IRE}}=4.0$, $k_{\text{film}}=0.5$,	

	Angles of Incidence=37, 39, 41, 43, 45, 47, and 49 Degree.....	48
4.4	Relationship Between Angles of Incidence and nk Values of Simulated Spectra with Small Absorption. The Spectra Used for Calculation were Those from Figure 4.2.....	49
4.5	Relationship Between Angles of Incidence and nk Values of Simulated Spectra with High Absorption. The Spectra Used for Calculation were Those from Figure 4.3.....	49
4.6	ATR Spectra of Nujol Acquired Via Ge IRE at 45-Degree Angle of Incidence.....	50
4.7	ATR Spectra of Nujol at 37, 39, 41, 43, 45, 47, and 49 Degree Angles of Incidence.....	51
4.8	Relationship Between Angles of Incidence and nk Values of Nujol. The Spectra Used for Calculation were Those from Figure 4.7.....	51
4.9	ATR Spectra of Uncrosslinked Chitosan Film (Mold-side) Acquired Via Ge IRE at 37, 39, 41, 43, 45, 47, and 49 Degree Angles of Incidence.....	54
4.10	ATR Spectra of Uncrosslinked Chitosan Film (Air-side) Acquired Via Ge IRE at 37, 39, 41, 43, 45, 47, and 49 Degree Angles of Incidence.....	54
4.11	Relationship between Angles of Incidence and nk Values of Uncrosslinked Chitosan Film (Mold-side). The Spectra Used for Calculation were Those from Figure 4.9.....	55
4.12	Relationship between Angles of Incidence and nk Values of Uncrosslinked Chitosan Film (Air-side). The Spectra Used for Calculation were Those from Figure 4.10.....	55
4.13	ATR Spectra of 10 Minutes Crosslinked Chitosan Film (Mold-side) Acquired Via Ge IRE at 37, 39, 41, 43, 45, 47, and 49 Degree Angles of Incidence..	59
4.14	ATR Spectra of 10 Minutes Crosslinked Chitosan Film (Air-side) Acquired Via Ge IRE at 37, 39, 41, 43, 45, 47, and 49 Degree Angles of Incidence.....	59
4.15	ATR Spectra of 100 Minutes Crosslinked Chitosan Film (Mold-side) Acquired Via Ge IRE at 37, 39, 41, 43, 45, 47, and 49 Degree Angles of Incidence.....	60

	Pages
4.16 ATR Spectra of 100 Minutes Crosslinked Chitosan Film (Air-side) Acquired Via Ge IRE at 37, 39, 41, 43, 45, 47, and 49 Degree Angles of Incidence.....	60
4.17 ATR Spectra of 1000 Minutes Crosslinked Chitosan Film (Mold-side) Acquired Via Ge IRE at 37, 39, 41, 43, 45, 47, and 49 Degree Angles of Incidence.....	61
4.18 ATR Spectra of 1000 Minutes Crosslinked Chitosan Film (Air-side) Acquired Via Ge IRE at 37, 39, 41, 43, 45, 47, and 49 Degree Angles of Incidence.....	61
4.19 Relationship between angles of incidence and nk values of 10 minutes crosslinked chitosan film (mold-side). The spectra used for calculation were those from Figure 4.13.....	62
4.20 Relationship between angles of incidence and nk values of 10 minutes crosslinked chitosan film (air-side). The spectra used for calculation were those from Figure 4.14.....	62
4.21 Relationship between angles of incidence and nk values of 100 minutes crosslinked chitosan film (mold-side). The spectra used for calculation were those from Figure 4.15.....	63
4.22 Relationship between angles of incidence and nk values of 100 minutes crosslinked chitosan film (air-side). The spectra used for calculation were those from Figure 4.16.....	63
4.23 Relationship between Angles of Incidence and nk Values of 1000 Minutes Crosslinked Chitosan Film (Mold-side). The Spectra Used for Calculation were Those from Figure 4.17.....	64
4.24 Relationship between Angles of Incidence and nk Values of 1000 Minutes Crosslinked Chitosan Film (Air-side). The Spectra Used for Calculation were Those from Figure 4.18.....	64
4.25 ATR Spectra of Chitosan Films (Mold-side) Crosslinked with Various Times Acquired Via Ge IRE at 39 Degree Angle of Incidence.....	65
4.26 ATR Spectra of Chitosan Films (Mold-side) Crosslinked with Various Times Acquired Via Ge IRE at 41 Degree Angle of Incidence.....	65

	Pages
4.27 ATR Spectra of Chitosan Films (Air-side) Crosslinked with Various Times Acquired Via Ge IRE at 39 Degree Angle of Incidence.....	66
4.28 ATR Spectra of Chitosan Films (Air-side) Crosslinked with Various Times Acquired Via Ge IRE at 41 Degree Angle of Incidence.....	66
4.29 ATR Spectra of 10 Minutes Crosslinked Chitosan Film Acquired Via Ge IRE at 39 Degree Angle of Incidence.....	67
4.30 ATR Spectra of 100 Minutes Crosslinked Chitosan Film Acquired Via Ge IRE at 39 Degree Angle of Incidence.....	67
4.31 ATR Spectra of 1000 Minutes Crosslinked Chitosan Film Acquired Via Ge IRE at 39 Degree angle of incidence.....	68

LIST OF TABLES

	Pages
2.1 Source of Chitin in Living Organisms.....	5
2.2 Solubility of Chitosan in Different Concentration of Various Types of Acid Solutions.....	10
2.3 Main Functions of Chitin and Chitosan, Their Applications and Utilization.....	13
2.4 Peak Assignments of Infrared Spectra of Glutaraldehyde, Chitosan and Chitosan Crosslinked by Glutaraldehyde.....	18
2.5 Comparing of Characteristics of Chitosan Specimen Crosslinked in Homogeneous and Heterogeneous System.....	21
4.1 Penetration Depth at Various Angles of Incidence of The Wavenumber Used to Calculate nk Values.....	53

สถาบันวิทยบริการ
จุฬาลงกรณ์มหาวิทยาลัย

LIST OF ABBREVIATIONS

ATR	: attenuated total reflection
Bp	: boiling point
d_p	: penetration depth
FT-IR	: Fourier transform infrared
Ge	: germanium
IRE	: internal reflection element
MSEF	: mean square electric field
MSEvF	: mean square evanescent field
ω	: wavenumber
ZnSe	: zinc selenide

LIST OF SYMBOLS

μ	: micro
-------	---------

สถาบันวิทยบริการ
จุฬาลงกรณ์มหาวิทยาลัย

CHAPTER 1

INTRODUCTION

Nowadays, chitosan is widely used in several applications including filtration, separation and medical applications. For such applications, chitosan is used as films. Film modification is a necessary process for altering the film properties to match the application. Crosslinking is a popular method for modifying chitosan film in order to improve tensile strength, solvent resistance, and filtration property. The properties of chitosan film are affected by several crosslinking parameters such as type and concentration of crosslinking agent, crosslinking time, crosslinking temperature, and crosslinking procedure. A number of crosslinking agents were reported to use with chitosan such as glutaraldehyde, sulfuric acid, and polyethylene glycol diglycidyl ether glyoxal have been employed.

Crosslinking procedure of chitosan film can be divided into two categories, homogeneous and heterogeneous crosslinking. For homogeneous crosslinking, crosslinking agent is mixed with chitosan solution. For heterogeneous crosslinking, chitosan in solid form (fiber, film, flake, or bead) is soaked in crosslinking agent. Heterogeneous crosslinking of chitosan film by using glutaraldehyde was reported in several researches.¹⁻⁸ Some researches indicated that this crosslinking condition bring about surface crosslinked films.^{7,9} In some reports, transmission technique was employed for investigate the crosslinking reaction.^{1,10} However, the real crosslinking densities at various depths of crosslinked film were not reported. It should be noted that the real crosslinking density must be known because it plays an important role in controlling the properties of the films. The properties of films are not modified if the crosslinking density is too small. However, high crosslinking density leads to film brittleness. In the surface crosslinked film, the crosslinking density is highest at the surface and decreases as a function of depth. If the crosslinking density of the surface is too high, the surface crack may occur. The defect causes drastically decrease the

mechanical property of the film. One can notice that the real crosslinking density of each layer of chitosan film is the important information, however, there is not yet any study on depth profiling of crosslinked chitosan film.

Surface characterization by ATR FT-IR spectroscopy is a well-known technique for characterizing the systems such as polymer composite, thin film, surface coating, chemical reaction, and diffusion. The process advantages of this technique are nondestructive, ease of sample preparation, fast and reliable. The use of ATR FT-IR spectroscopy as a depth profiling technique was introduced in 1992. ATR FT-IR spectroscopy was used to observe the degree of saponification of diacetyl cellulose film coated on poly (ethylene terephthalate). The ATR spectra, acquired from different angles of incidence, indicated the non-uniform distribution of functional groups in the depth direction at a few micrometers from the surface. After that, ATR FT-IR spectroscopy was used for the determination of depth dependent property by several research works.¹¹⁻¹⁴

The objective of this research is to determine the crosslinking density at various depths of chitosan films that have been crosslinked by dipping in glutaraldehyde solution. The technique used to determine the crosslinking density was attenuated total reflection Fourier transform infrared (ATR FT-IR) spectroscopy. By varying the angle of incidence and performing mathematical operation on the observed spectra, the information at various depths of the films in terms of nk values were achieved.

CHAPTER 2

THEORETICAL BACKGROUND

2.1 Chitosan

2.1.1 Introduction

Chitin and chitosan are natural biopolymer. From structural point of view, they are basically cellulose derivatives. By substituting hydroxy (-OH) group at C2 in cellulose by acetamido group (-NH-CO-NH₂) chitin (poly β -(1-4)-2-acetamido-2-deoxy-D-glucose) is obtained. If acetamido groups are partially substituted by amine groups (-NH₂), the molecular structure of chitosan (poly (β -(1-4)-2-amino-2-deoxy-D-glucose) is obtained. Molecular structure of cellulose, chitin and chitosan are shown in Figure 2.1. Chitin and chitosan can be found in nature but in different quantity. Chitin is the second natural abundance biopolymer after cellulose. Chitosan exist in nature in only little amount compared to chitin. The source of chitin and chitosan are shown in Table 2.1.

The serious drawback of chitin is its solubility property. To dissolve chitin, one has to employ hazardous solvent whereas chitosan, on the other hand, can be dissolved in less corrosive or mild solvent, such as dilute acetic acid. From the economical point of view, most of chitosan is made from chitin, which is the waste of seafood industries.

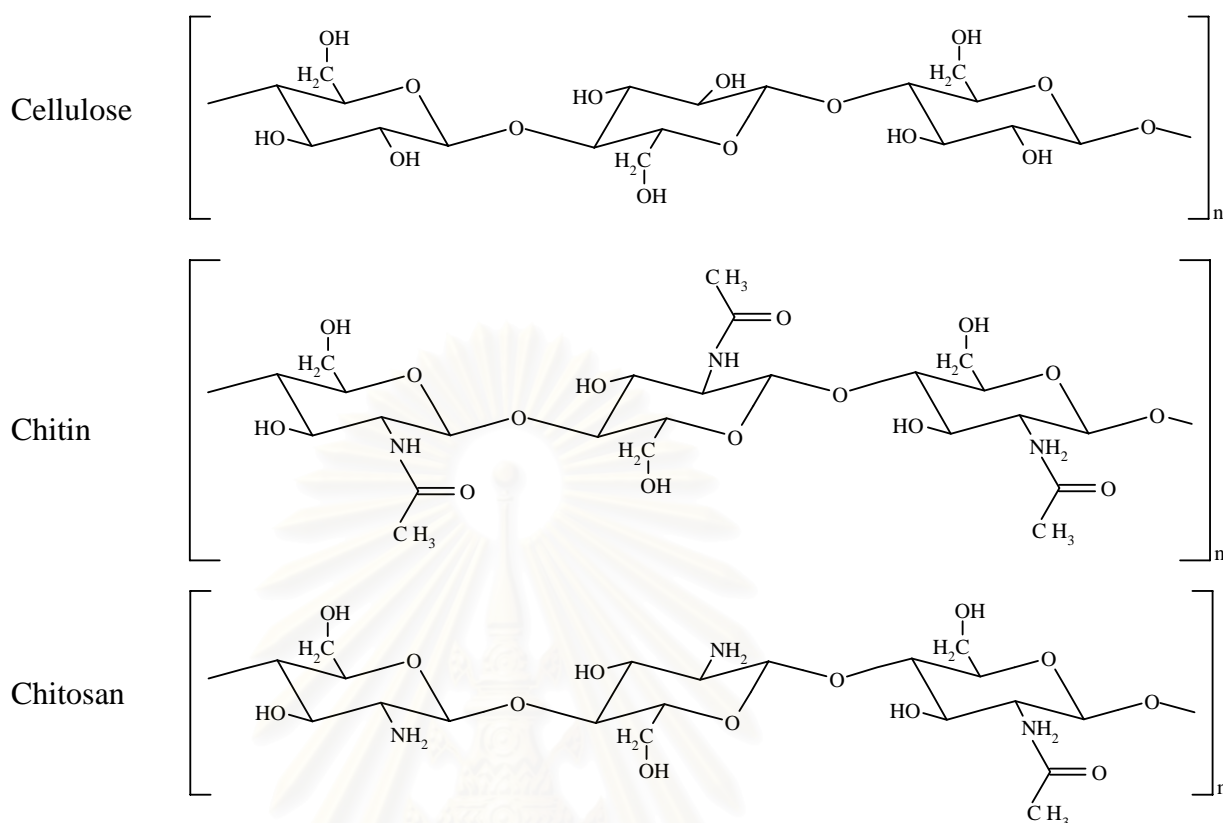


Figure 2.1 Structures of cellulose, chitin, and chitosan.

2.1.2 Chitin Manufacturing Process.

In crab or shrimp shell, apart from chitin, there are other compositions: minerals (calcium carbonate), proteins, and pigments. The key steps in extracting chitin from shells are to remove proteins and minerals by alkali and acid treatment. First, proteins are removed from ground shell by sodium hydroxide. Minerals are then extracted by using hydrochloric acid. After rinsing, the chitin is left dry as a flake material. The process for chitin production is shown below.

Table 2.1 Source of chitin in living organisms

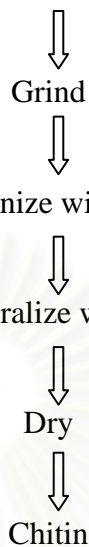
Organism	Structure	Chitin		Other components	
		% Organism fraction	Crystal type	Inorganic	Organic
FUNGI					
<i>Ascomyceta</i> <i>Basidiomyceta</i> <i>Phycomyceta</i> <i>Imperfecti</i>	cell walls and structural Membranes of mycelia, stalks and spores	traces-45		--	polysaccharides such as glucans or mannans
ALGAE					
<i>Chlorophyceae</i>	cell wall	+	-	--	cellulose
PROTOZOA					
<i>Rhizopoda:</i>					
<i>Pelomyxa</i>	cyst wall	+	-	--	--
<i>Plagiopyxidae</i>	shell	+	-	silica	--
<i>Allogromia</i>	shell	+	-	iron	proteins and lipids
<i>Ciliata</i>	cyst wall	+	-	--	proteins
CNIDARIA					
<i>Hydrozoa:</i>					
<i>Hydroidea</i>	perisarc	+	α	--	--
<i>Milleporina</i>	coenosteum	+	α	CaCO ₃	--
<i>Siphonophora</i>	pneumatophore	+	-	--	proteins
<i>Anthozoa</i>	skeleton	+	-	CaCO ₃	proteins
<i>Scyphozoa</i>	podocyst	+	-	--	proteins
ASCHELMINTHES					
<i>Rotifera</i>	egg envelope (inner membrane)	14.6	-	--	proteins
<i>Nematoda</i>	egg capsule (middle membrane)	16.6	-	--	proteins
<i>Acanthocephala</i>	egg capsule	+	-	--	--
<i>Priapulida</i>	cuticle	+	-	--	tanned proteins
ENDOPROCTA					
	cuticle	+	-	--	tanned proteins
BRYOZOA					
	ectocyst	1.6-6.4	-	CaCO ₃	proteins
PHORONIDA					
	tubes	13.5	-	--	proteins
BRACHIOPODA					
<i>Articulata</i>	stalk cuticle	3.8	-	--	--
<i>Inarticulata</i>	stalk cuticle	+	γ	--	collagen
	shell	29.0	β	CaCO ₃	--
ECHIURIDA					
	hooked chaetae	+	-	--	--
ANNELIDA					
<i>Polychaeta</i>					
	chaetae	20.2-38.0	β	--	quinone-tanned proteins
<i>Oligochaeta</i>	jaws (Eunicidae)	0.28	-	unidentified	proteins
<i>All</i>	chaetae; gizzard cuticle	+	β	--	--
	peritrophic membrane	+	-	--	proteins

Table 2.1 Source of chitin in living organisms (continue)

Organism	Structure	Chitin		Other components	
		% Organism fraction	Crystal type	Inorganic	Organic
MOLLUSCA					
<i>Polyplacophora</i>	shell plates; mantle bristles	12.0	-	CaCO ₃	proteins
	radula	+	-	iron	proteins
<i>Gastropoda</i>	shell (mother of pearl)	3.0-70	-	CaCO ₃	conchiolin
	radula	19.7	-	iron and silica	tanned proteins
	jaws	+	-	--	tanned proteins
	`stomachal plates` (Opisthobranchia)	36.8	-	--	tanned proteins
<i>Cephalopoda</i>	Calcified shell	3.5-26.0	β	CaCO ₃	conchiolin
	`pen` (Loligo, Octopus)	17.9	β	--	`conchagen`
	jaws and radula	19.5	α	--	tanned proteins
	stomach cuticle	-	γ	--	--
<i>Lamellibranchia</i>	periostracum	0.7-3	-	CaCO ₃	proteins
	prisms	traces-0.2	-	CaCO ₃	conchiolin
	shell mother of pearl	0.1-1.2	-	CaCO ₃	conchiolin
	calciostacum	0.2-8.3	-	CaCO ₃	conchiolin
	gastric shield	17.3	-	CaCO ₃	--
				--	
ONYCHIOPHORA	cuticle	+	-	--	proteins
ARTHROPODA					
<i>Crustacea</i>	calcified cuticle	58.0-85.0	α	CaCO ₃	arthropodins+ sclerotins (10-32%)
<i>Diplopoda</i>	intersegmental membranes	48.0-80.0	α	--	arthropodins (23-51%)
<i>Insecta</i>	hardened cuticle	20.0-60.0	α	--	arthropodins+ sclerotins (40-76%)
<i>Arachnida</i>					
<i>Chilopoda</i>	unhardened cuticle	20.0-60.0	α	--	arthropodins+ (in some parts) resilin
<i>All</i>	peritrophic membrane	3.8-22.0	-	--	protein21-475 +mucins
CHAETOGNATHA	grasping spines	+	-	--	--
POGONOPHORA	tubes	33.0	β	--	proteins(47%)
TUNICATA	peritrophic membrane	+	-	--	--

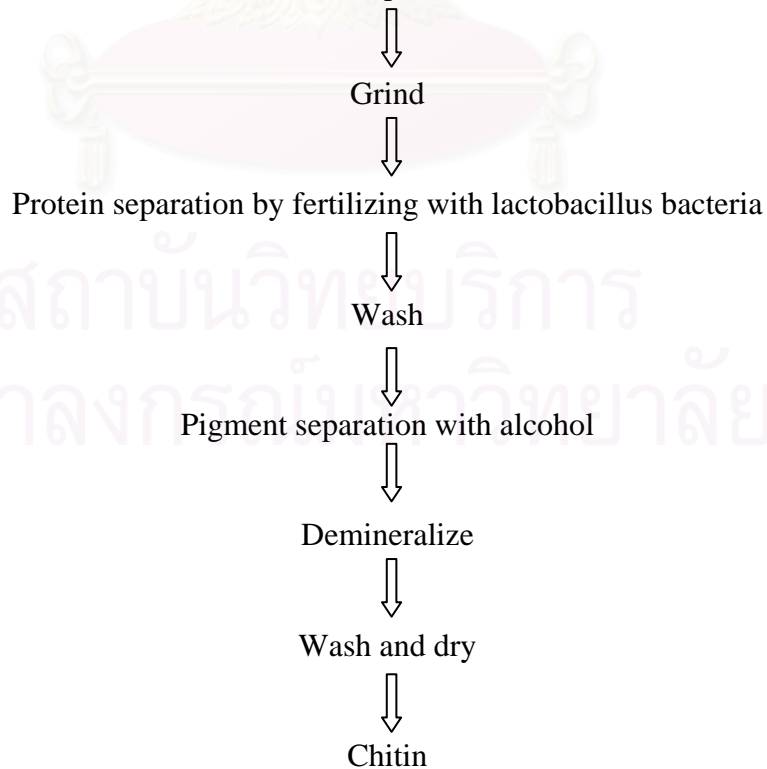
Source: Roberts, G.A.F. (1992), Structure of chitin and chitosan, *Chitin Chemistry*, Macmillan, pp.2-4

Raw material: crab or shrimp shells



Some different process and auxiliary treatments in chitin manufacturing process have also been reported by using biotechnology process which more environmental friendly.^{15,16}

Shrimp shell



2.1.3. Chitosan Manufacturing Process

Chitin is changed to chitosan by deacetylation reaction with concentrated alkali at high temperature. Variation on the reagents used and their concentration, as well as time and temperature of treatment determine the properties and characteristics of the product. The manufacturing of chitosan is documented in many literatures.¹⁵⁻²⁰ The parameters that influence chitin deacetylation includes:

1. Type of reagent
2. Concentration of reagent
3. Chitin-reagent ratio
4. Size of chitin particles
5. Reaction temperature
6. Reaction time
7. Reaction atmosphere

2.1.4. Characteristics of Chitosan

The empirical formula of chitosan is $(C_6H_{11}O_4N)_n$ with molecular weight 161 for monomer and 10,000-10,000,000 for polymer. Chitosan is tasteless, odorless, with white to cream flake. It has pKa of 6.3-6.7. Chitosan is incompatible with anionic and aldehyde substances. It is hygroscopic and should be kept in well-closed container. Some important properties of chitosan are briefly mentioned as the following:

1. Molecular Weight

Natural chitin has molecular weight more than 1,000,000, whereas, molecular weight of chitosan is between 50,000-4,000,000 depended on the processing condition. The average molecular weight of chitosan is the most difficult parameter to control.

2. Degree of Deacetylation

Chitosan does not refer to a homopolymer but copolymer containing two monomer residues, anhydro-N-acetyl-D-glucosamine and anhydro-D-glucosamine. The former is the predominant component in chitin while the latter is the predominant component in chitosan. Usually, chitosan has degree of deacetylation between 70 and 90 %. Properties of chitosan are greatly affected by the degree of deacetylation.^{17-19, 21} As a consequence of the influence of this parameter on the properties of chitosan, numerous methods for determination the degree of deacetylation were proposed such as titration, NMR, and FT-IR spectroscopy.^{15, 22-29} It should be noted that IR technique is widely used because of its ease and the other methods can be used to confirm the IR spectroscopic test.

3. Solubility

Chitosan is insoluble in water, alcohol, base, and organic solvents while soluble in almost every organic acid solution with pH less than 6. Since chitosan is a cationic polymer having a pKa of 6.3, its solubility depends on the presence of the free amine groups capable of being protonated by the acid medium. The exact degree of deacetylation required to render a polymer soluble is not readily determined, and undoubtedly varied to such factors as chitosan molecular weight, concentration, impurity, and nature of the acid employed.

For practical purpose, chitosan is insoluble in sulfuric acid and phosphoric acid at room temperature, while certain solubility exists for other mineral acids like hydrochloric acid, nitric acid and perchloric acid. Comparing with the more common organic acids, the solubility in inorganic acids seems more limited concerning the concentration ration chitosan/acid. The solubility of chitosan in some organic acid is up to 50% such as acetic acid, lactic acid, formic acid, and propionic acid. The standard solvent commonly used for solution property measurement is acetic acid. Chitosan solution is viscose, transparent and non-Newtonian. The pKa of chitosan is in about 6.2-6.8 depending on charge density on polymer chain³⁰. Solubility

parameter of chitosan (%DD=64) is 37.0-43.5.³¹ Solubility of chitosan in different types of acid solutions is shown in Table 2.2.

Table 2.2 Solubility of chitosan in different concentration of various types of acid solutions.

Acid types	Concentration of acid solution (v/v)				
	1%	5%	10%	50%	>50%
Acetic	+	+	+	+	
Adipic	+				
Citric	-				
Formic	+	+	+	+	+
Lactic	+	+	+		
Malic	+	+	+		
Tartaric	-		+		
Hydrochloric	+	-	-		
Nitric	+	-	-		
H ₃ PO ₄ *	-	-	-		
Sulfuric	-	-	-		

Note: + Soluble

- Insoluble

* Insoluble in sulfuric acid solution and phosphoric acid solution but soluble in phosphoric acid solution at concentration less than 0.5%

4. Viscosity

Viscosity of chitosan solution depends on several factors such as degree of deacetylation, molecular weight, ionic strength, concentration, pH, the added salt concentration and temperature.

The viscosity increases with an increase in molecular weight and concentration of chitosan. The viscosity is increased with increasing temperature. The addition of salt reduces the repelling effect of each positively charged deacetylated unit on neighboring glucosamine unit and will reduce an extended conformation of the polymer in solution. This effect resulting in a more random coil like conformation of the molecule will decrease the viscosity of chitosan solution. However, the acid type and pH changing may result in the different in viscosity. For

example, viscosity of chitosan solution in acetic acid increases when pH is decreased, while in hydrochloric acid, viscosity of chitosan solution increases when pH is increased.

5. Rheology

Chitosan solution behaves as a pseudoplastic material which viscosity decreased when shear increased.

6. Coagulation Ability

Chitosan is a good flocculant and coagulation agent because amino group can be protonated to positive charge. As a result, chitosan can bind with molecules containing negative charge such as proteins, dyes, and other polymers. Moreover, chitosan can form complex with metal since nitrogen behaves as electron donor. One can see that amine group is the key functional group in coagulation ability, thus, coagulation ability increases when degree of deacetylation increases.

7. Degradation

Chitosan is like other polymers that it can be degraded to smaller molecules, oligomer and monomers. Degradation of chitosan occurs in various reactions such as:

- acid hydrolysis
- alkaline degradation or peeling reaction
- degradation by sonication
- enzymic degradation
- thermal degradation

8. Active Groups

Chitosan molecule contains three active functional groups, those are amino group ($-NH_2$), primary hydroxy group ($-CH_2OH$) and secondary hydroxy group ($-CHOH$). As a result, chitosan can be chemically modified to fit in the wide range of application.

9. Toxicity

Chitosan is biopolymer, therefore, it is not toxic to human. However, consumed chitosan will be evacuated out of human body since there is no enzyme for chitosan digestion in human body.

2.1.5 Applications

The used of chitosan has been reported to use in several applications. Some of them are shown in Table 2.3

สถาบันวิทยบริการ
จุฬาลงกรณ์มหาวิทยาลัย

Table 2.3 Main functions of chitin and chitosan, their applications and utilization

Function*	Applications and Utilization*
1. Polyelectrolyte and chelate (B)	1. <u>Coagulant, flocculating agents and cationic for polluted waste water</u> ; 2. Recovery of <u>acidic proteins</u> , Uranium, specific metal ions and radioactive isotope in water
2. Molding or casting (A, B)	1. <u>Fibers, textiles, non-woven fabrics</u> etc.; 2. Membranes: permeation, filter, separation of water and alcohol etc.; 3. <u>Beads</u> , capsules, media for cell culture etc.
3. Hydrogelation (B)	1. Immobilization of cells, enzymes, etc.; 2. Media for gel chromatography; 3. <u>Sponge sheets</u> ; 4. Xerogels
4. CO ₂ -fixation (A, B)	CO ₂ fixation in hydrosphere, CO ₂ composite materials
5. Hydrolysis (A, B)	<u>D-Glucosamine, oligosaccharides</u> (chemical and enzymatic)
6. Viscous and moisturizing (B)	1. <u>Cosmetic ingredients for skin and hair cares</u> ; 2. A thickener for food process and manufacture; 3. Improvement of food properties
7. Molecular affinity (A, B, C)	Media for affinity chromatography of wheat lectin, chitinase and lysozyme, and for ion-exchange chromatography
8. Molecular reactions	1. Flavoring; 2. Deodorant of formaldehyde etc.; 3. Synthetic materials for other functional compounds (<u>CM-chitin, HE-chitin</u> , muraminan etc.)
9. Conductance (B)	Chitosan film-lithium triflate electrolyte in battery
10. Coating (B)	1. <u>Paint, print and dyeing additives</u> ; 2. Paining; 3. Speaker, music instruments; 4. An additive for paper manufacturing
11. Elicitor (A, B, C)	1. An induction of pathogenesis-related (PR) proteins; 2. <u>Agricultural materials</u> (plant seed coating, leaf surface sprinkling etc.)
12. Antibacterial (B)	Storage of foods and fruits
13. Microbial flora-control	Improvements of microbial flora 1. In the soil and hydrosphere; 2. In animal and human intestines
14. Nontoxic	Biologically friendly applications
15. Biological defense (immunological)-enhancing (A, B, C)	1. Introduction of lysozyme and LPL activities in tissues and bloods; 2. Anti-cancer agent
16. Wound healing (A, B, C)	1. <u>Wound dressing materials for burn and skin lesion for animals and humans</u> and for trees. (artificial skin); 2. Bone, tendon and ligament repairing
17. Biodegradable (A, B, C)	1. <u>Absorbable surgical sutures</u> ; 2. The sustained vehicles of drugs; 3. The control of enzymatic hydrolysis rate by the structure and d.s.of N-and O-substituent groups
18. Hypocholesteromic (B)	1. <u>Health food and feed additives</u> ; 2. Decrease in blood pressure
19. Hemostatic (B)	Heparinioids
20. Antithrombogenic (C)	1. Blood vessel, contact lens etc. for N-hexanoyl and N-octanoylchitosans; 2. Preservation of the freshness of fruits, vegetables, aggs etc.
21. Biocompatibility (A, B, C)	1. <u>Wound-dressing</u> ; 2. <u>Sutures</u>

* A:Chitin, B:Chitisan and C:Drivatives

* The current commercial applications are underlined.

Source: Chitin and chitosan technical note (No.1), Metakanon P. et al. (2000),

MTEC, pp.1-2

2.2 Crosslinking of Chitosan

2.2.1 Background

Crosslinking is one of the most popular methods being used to modify chitosan in order to achieve desired properties. Some properties could be altered by crosslinking such as swelling^{3,8-9}, permeability⁴⁻⁶, drug releasing^{10,32}, transport properties¹, water uptake⁶, mechanical properties^{6,9}, chemical stability⁸, sponge structure³, and Crystallinity.³³

It should be noted that the properties achieved are strongly depending on crosslinking procedure (i.e., crosslinking agent, crosslinking condition, crosslinking technique). Several crosslinking agents for chitosan are employed such as glutaraldehyde^{1,3,32,34,35}, sodiumtripolyphosphate³⁶, genepin³⁷, copper sulfate³⁸, calcium chloride³⁹, ethylene glycol diglycidyl ether⁴⁰, and sulfuric acid.^{35,41} However, the most popular crosslinker is glutaraldehyde. Glutaraldehyde is a small molecule dialdehyde. Its chemical information is given below.

Glutaraldehyde

Other name: pentane dial, glutaral, glutaric dialdehyde, and 1,3-diformylpropane

Molecular structure: $\text{OHC}(\text{CH}_2)_3\text{CHO}$

Molecular weight: 100.11

C = 59.98% H = 8.05% O = 31.97%

Bp₇₆₀ = 187-189 °C

Bp₅₀ = 106-108 °C

Bp₁₀ = 71-72 °C

Refractive index (25 degree) = 1.4338

2.2.2 Crosslinking Reaction of Chitosan

2.2.2.1 Crosslinking Reaction with Glutaraldehyde

Crosslinking reaction between chitosan and glutaraldehyde occurs from amine group of chitosan and aldehyde group of glutaraldehyde. (as shown in Figure 2.2)

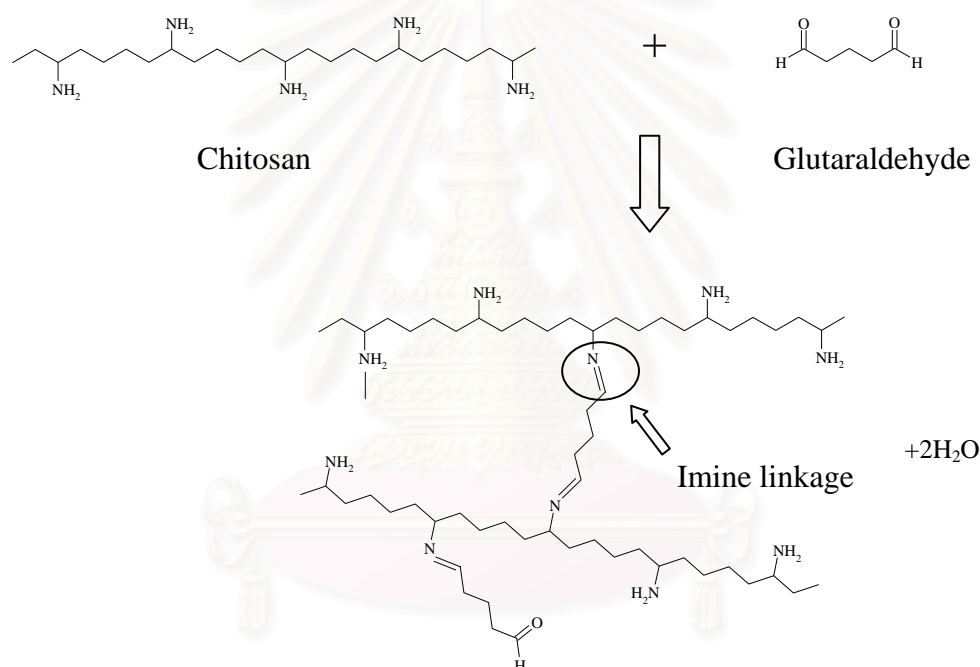


Figure 2.2 Crosslinking reaction between chitosan and glutaraldehyde

Although imine linkage is mainly formed in the crosslinking reaction, different mechanisms have been proposed in order to explain the crosslinking reaction between chitosan and glutaraldehyde¹,

1. Schiff's base formation has been proposed and leads to the formation of imine-type crosslinked according to Figure 2.3(A)

2. Michael-type adducts with amine groups leading to the type of crosslinked proposed by Muzzarelli have also been considered. They lead to the presence of carbonyl groups on the polymer structure. (Figure 2.3 (B))
3. In addition to these crosslinking phenomena, the formation of oligomers presented in Figure 2.3(C) is also proposed.

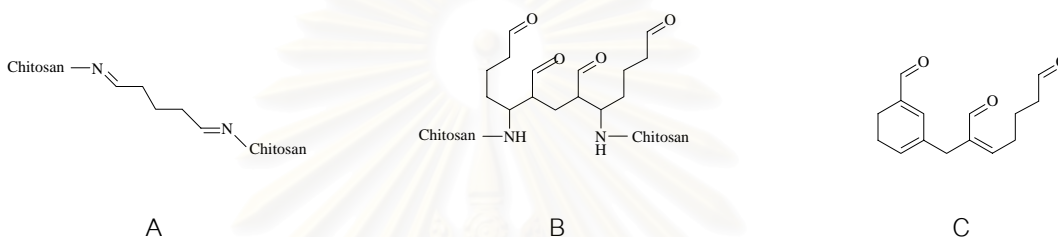


Figure 2.3 Proposed structure for chitosan crosslinked by glutaraldehyde¹

Crosslinking reaction of chitosan with glutaraldehyde is easily observed by Infrared spectroscopic technique. The most popular sampling technique is transmission. However, ATR technique is also be used in order to determine the surface properties. IR spectra of chitosan, glutaraldehyde and chitosan crosslinked with glutaraldehyde are shown in Figure 2.4.

There are many infrared absorbance peaks related to crosslinking reaction between chitosan and glutaraldehyde. The peaks at 1655 and 1564 cm^{-1} are the most used due to their high absorptivity. Crosslinking reaction leads to decreasing of peak height at 1564 cm^{-1} , which indicates amine group, and increasing of peak height at 1655 cm^{-1} , which indicates imine group. Peak assignment of the spectra is listed in Table 2.4

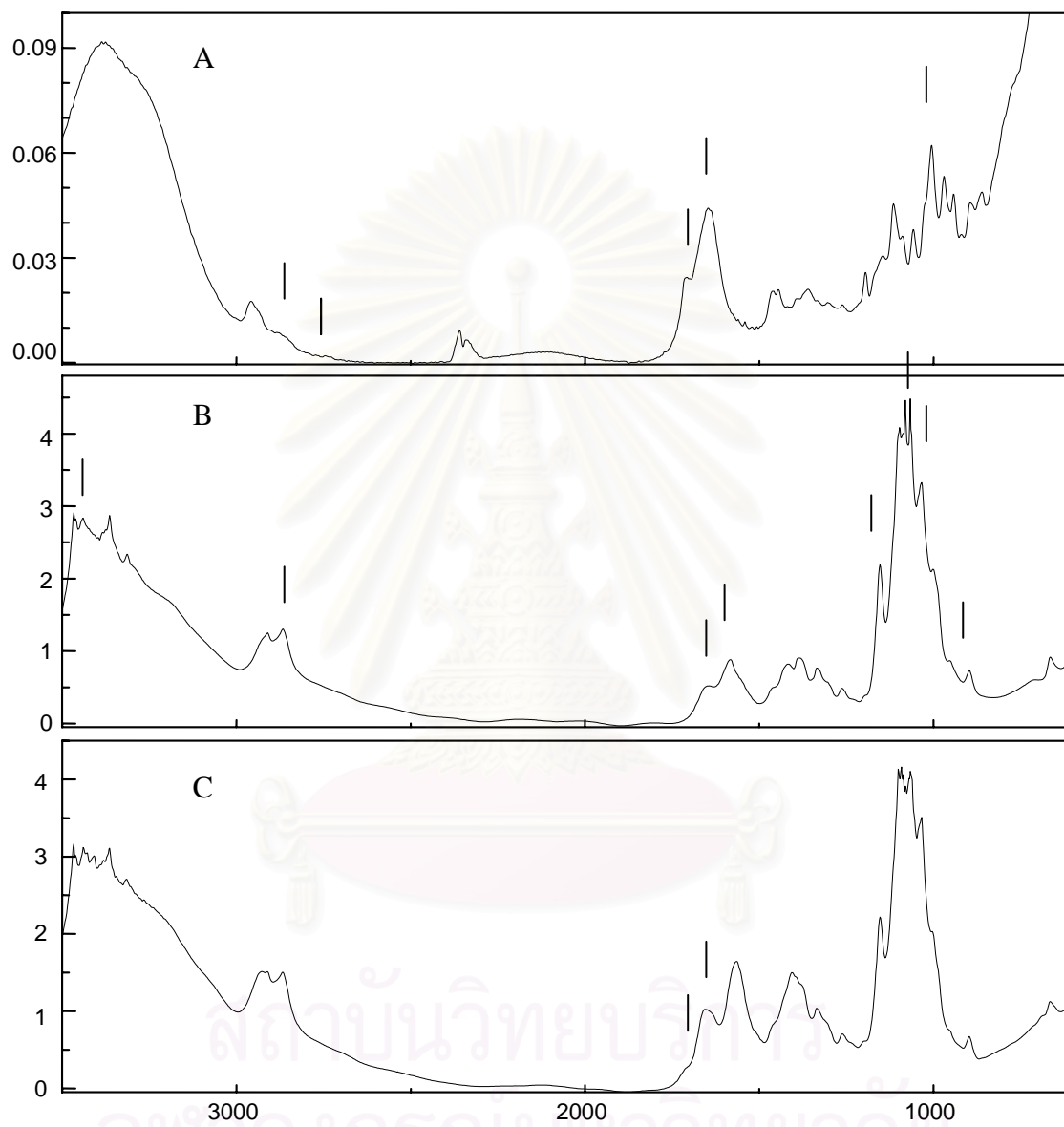


Figure 2.4 Infrared spectra glutaraldehyde (A), chitosan (B) and crosslinked chitosan (C)

Table 2.4 Peak assignments of infrared spectra of glutaraldehyde, chitosan and chitosan crosslinked by glutaraldehyde

Peak (cm ⁻¹)	Possible assignment
Glutaraldehyde	
2740,2855	C-H stretching vibration
1706	C=O stretching vibration
1645	C=O stretching vibration (shift by conjugating)
1114	C-O stretching vibration of trimer or polymer
Chitosan	
3453	O-H stretching vibration
2870	C-H stretching vibration
1652	C=O stretching vibration
1584	C-N stretching vibration
1564	N-H bending vibration
1153	C-O stretching vibration (asymmetric oxygen bridge)
1066	C-O stretching
1035	C-O stretching
897	ring stretching
Chitosan crosslinked by glutaraldehyde	
1707	C=O stretching vibration
1645	C=N stretching vibration of imine group

2.2.2.2 Crosslinking Procedure of Chitosan with Glutaraldehyde

Crosslinking reaction between chitosan and glutaraldehyde depends on temperature, concentration of chitosan, concentration of glutaraldehyde, and the employed acid. Moreover, crosslinking procedure plays important roles in chitosan properties. Crosslinking procedure of chitosan with glutaraldehyde can be separated into two categories.

1. Homogeneous crosslinking.^{32, 33, 42} In this procedure, glutaraldehyde is mixed into chitosan solution.
2. Heterogeneous crosslinking.¹⁻⁸ In this procedure, chitosan in solid form (fiber, film, flake, or bead) are soaked in glutaraldehyde solution.

The characteristics of chitosan specimens, which were crosslinked in each procedure, are compared in **Table 2.5**. From **Table 2.5**, solution crosslinking procedure is easier than solid crosslinking, however, there are some limits of solution crosslinking. In case that there are other chemicals mixing in the solution (i.e., porogen, plasticizer), the crosslinking reaction may be disturbed resulting in difficult to control the extent of reaction. In this case, one can use solid crosslinking process to avoid undesirable reaction. Crosslinking agent of chitosan can be divided into two categories.⁴³ One is small molecules crosslinking agent (such as glutaraldehyde, glyoxal, succinaldehyde, trichlorotriazine, epihalohydrin, benzoquinone and bisepoxiranes. This type of crosslinking agent can penetrate into chitosan matrix, so crosslinking reaction occurred not only at the chitosan surface but also in the chitosan matrix. The other is large molecule crosslinking agent such as dextran dialdehyde, starch dealdehyde, dealdehyde of caragenan and dialdehyde of alginic acid. This type of crosslinking agent can react only at the chitosan surface because of their high molecular weight.

The influence of crosslinking on transport properties of chitosan membranes was studied.¹ Chitosan membranes were crosslinked by solid crosslinking process with different crosslinking time. Transmission infrared spectroscopy was used to confirm crosslinking reaction. Crosslinking reaction was confirmed by the present of adsorption band at peak 1662 and 1723 cm^{-1} . The degree of crosslinking was calculated from the different of the weight of sample after and before crosslinking. It should be noted that the crystalline phase was not affected by crosslinking reaction. The result was degree of crosslinking increased as a function of time. Moreover, if the crosslinking time is less than 5 hours, crosslinking reaction occurs through a Schiff's base formation.

In the research where chitosan fibers were crosslinked by submerging in glutaraldehyde solution, on IR microscope, they observed that the crosslinking reaction proceeds only to a minimal depth below the fiber surface.⁹ However the majority of the core is never affected. The yarn count of chitosan fiber in this experiment is 20.67 decitex or 18.62 denier.

The effect of crosslinking on sieving characteristics of chitosan composite membranes was studied.⁷ Chitosan film, 0.5 μm thick, was formed onto poly(acrylonitrile) membrane and then was crosslinked by using glutaraldehyde solution. They believed that crosslinking reaction took place only on the exterior surface of chitosan, because glutaraldehyde molecules could not diffuse inside after exterior surface was crosslinked.

Table 2.5 Comparing of characteristics of chitosan specimen crosslinked in homogeneous and heterogeneous system.

Property	Homogeneous crosslinking	Heterogeneous crosslinking
distribution of crosslinker in chitosan	good distribution because crosslinker can be dispersed easily in chitosan solution	depend on diffusability of crosslinker into swelling chitosan matrix(so, every diffusion parameter effected crosslinker distribution)
ratio between crosslinker and chitosan	easily, by mixing known amount of crosslinker with chitosan solution	difficult because some of crosslinker in crosslinking solution not react with chitosan
procedure	more easy, only mix crosslinker into chitosan solution	more steps, such as dipping, crosslinking solution preparation
crystallinity	less crystallinity, because crystal forming of chitosan molecules are more difficult after crosslinked	more crystallinity, because crosslinking reaction occurred only in amorphous region, not disturb crystalline region

2.3 Infrared Spectroscopy

2.3.1 Basic Concepts of Spectroscopy

Spectroscopy is a study of the interactions of electromagnetic radiation with matters. After the electromagnetic radiation impinges on the surface of an object, the interaction between the incident beam and the molecules of object occurs. This interaction alters the incident beam and causes reflected, scattered, transmitted or absorbed incident radiation. Thus, this altered radiation can bring out the information and properties of the object.

Light is an electromagnetic wave of which the electric and magnetic vectorial components are perpendicular to each other and to the direction of propagation.

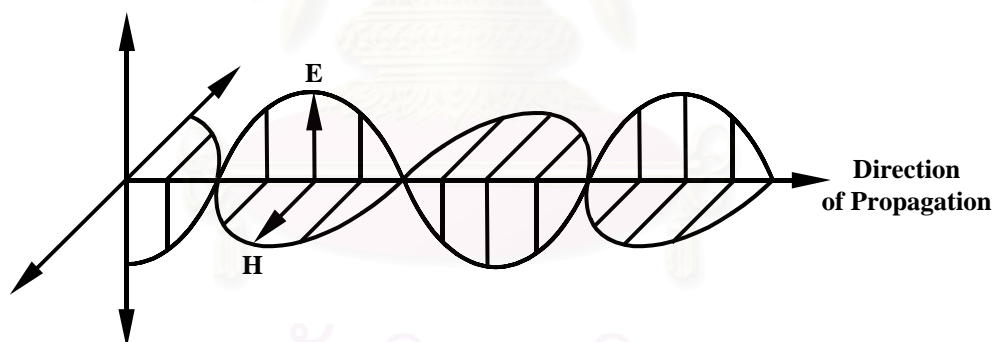


Figure 2.5 Propagation of a linearly polarized electromagnetic wave in the direction of propagation.

When electromagnetic radiation impinges on a matter, the incident beam can be reflected, transmitted, scattered or absorbed as shown in **Figure 2.6**. The total amount of incident intensity is the sum of reflected, scattered, transmitted, and absorbed intensities. This can be expressed by:

$$I_0 = I_R + I_S + I_T + I_A \quad (2.1)$$

where I_0 , I_R , I_S , I_T , and I_A is the intensity of the incident, reflected, scattered, transmitted, and absorbed beams, respectively. The factors affected these beam intensities are the intensity and wavelength of the incident beam, the properties of the specimen, and the experimental condition.

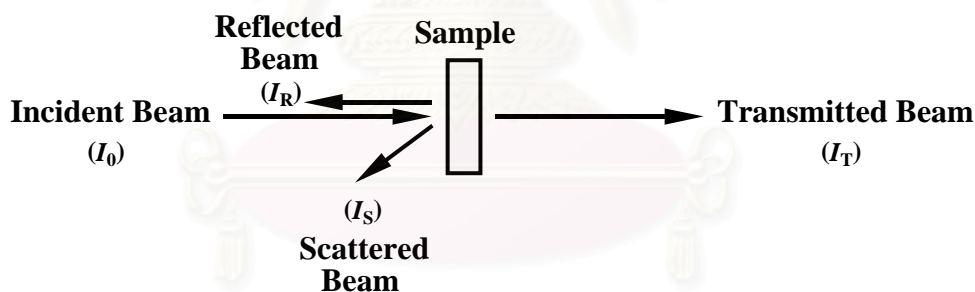


Figure 2.6 Interactions of light with matter.

When a sample is placed between the light source and the detector, a fraction of the incident radiation is absorbed by the sample. In order to measure the amount of the absorbed light, the ratio of the sample attenuated (I), and nonattenuated (I_0) intensities of the radiation are needed. The ratio is proportional to the transmittance of the sample. This relationship is quantitatively related to the chemical composition of the sample by the Beer-Lambert law as

$$I / I_0 = e^{-A(\nu)} = e^{-c_2 \varepsilon(\nu) l} \quad (2.2)$$

where $A(\nu)$ is the sample absorbance at a given wavenumber ν , c_2 is the concentration of the absorbing functional group, $\varepsilon(\nu)$ is the wavenumber-dependent absorption coefficient, and l is the film thickness for the IR beam at a normal incidence to the sample surface.

By using transmission technique as described above, several informations of molecular structures and properties of samples are achieved. By the way, there is limitation of transmission technique. If one wants to gain the surface properties of sample, transmission technique cannot be used because it brings about bulk properties of the specimen. For this propose, ATR FT-IR is a more suitable technique since it can provide surface information of the sample.

2.3.2 Reflection and Refraction

Both refraction and reflection occur in the system that electromagnetic radiation impinges the boundary of two transparent media with different refractive indices. The difference between reflection and refraction is that in reflection light still travels in the original medium after strike the interface, while in refraction, light travels pass the first medium into the second medium. There is direction change in both reflection and refraction. However, the law given for each case is not the same. In reflection, the angle of incidence is equal to the angle of reflection (**Figure 2.7**). In refraction, the direction of radiation is given by the following equation

$$\frac{\sin \alpha_1}{\sin \alpha_2} = \frac{n_2(\nu)}{n_1(\nu)} \quad (2.3)$$

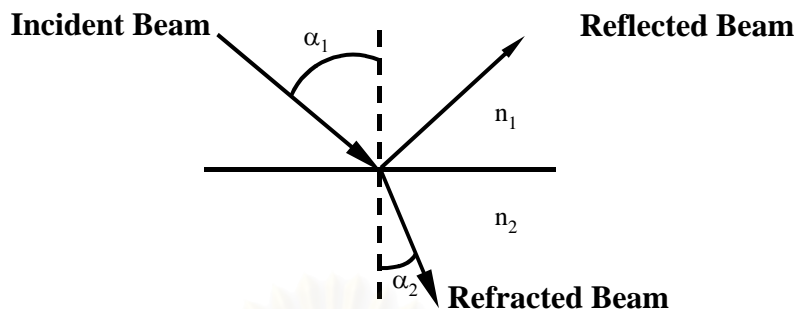


Figure 2.7 Reflection and refraction at the interface of two media with different refractive index. In this case $n_1 < n_2$

where α_1 and α_2 are the angle of incidence and the angle of refraction, respectively. If electromagnetic radiation passes from one medium to another that has a different refractive index, a sudden change of beam direction occurs since the difference in propagation velocity through two media. By increasing the angle of incidence, when $n_1 > n_2$, the angle of refracted beam is increased until the angle of incidence reaches critical angle (θ_c), the angle of incidence that gives the angle of refraction of 90 degree (**Figure 2.8**). From θ_c , any further increment of incident angle will not cause refraction but total reflection. The critical angle can be derived from Snell's law and given by the following equation:

$$\theta_c = \sin^{-1}(n_2(v) / n_1(v)). \quad (2.4)$$

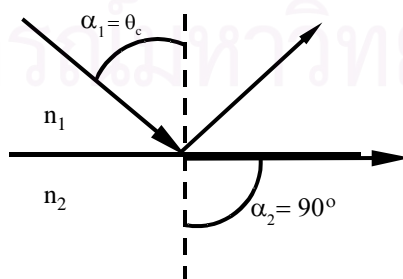


Figure 2.8 Reflection and refraction at critical angle

It should be noted that under a total internal reflection, there is no radiation from the optically denser medium (n_1) travels across the boundary into the optically rarer medium (n_2), $n_1 > n_2$.

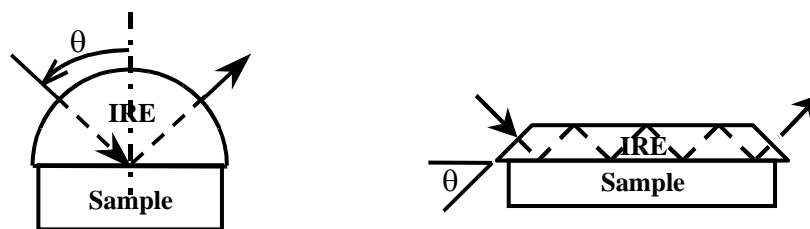
2.3.3 ATR FT-IR Spectroscopy

2.3.3.1 Introduction

Attenuated total reflection Fourier transform infrared spectroscopy (ATR FT-IR) is a characterization technique using an internal reflection principle, look at 2.1.2. This optical phenomenon, total internal reflection, can be easily observed in everyday life. For example, with a glass of water, if the side of the glass below the water level is viewed obliquely through the water surface, it appears to be silvered and objects behind it cannot be seen. This results from that light, which impinges the glass surface, is completely reflected, therefore, the objects behind the glass surface cannot be seen.

2.3.3.2 Internal Reflection Elements (IRE)

The internal reflection element (IRE) is an important part of ATR accessories. IRE is made from high refractive index and infrared transparent material such as zinc selenide (ZnSe) crystal, germanium (Ge) crystal, KRS-5 or cadmium telluride, etc. The IRE configurations commonly used in ATR accessories are single reflection variable-angle hemispherical or hemicylindrical crystals, and multiple reflection single-pass crystals (**Figure 2.9**). ATR spectra are obtained easily by placing the sample against the IRE. The information obtained from the spectrum is dependent on several factors such as characteristics of the IRE, angle of incidence, number of reflections, aperture, number of passes, surface preparation, sample-IRE contact, and the material of which the sample is made.



a.) Single Reflection

b.) Multiple Reflections

Figure 2.9 Selected IRE configurations commonly used in ATR experimental setups: a.) Single reflection variable-angle hemispherical or hemicylinder crystal, and b.) Multiple reflection single-pass crystal.

2.3.3.3 Variable Angle Accessories (Seagull™)

The IRE configuration used in this research is single reflection variable-angle hemispherical crystal made of germanium. IRE is equipped in a multifunctional variable-angle reflection attachment, Seagull™. By using this accessory, the angle of incidence can be adjusted from 5 to 85 degree. A schematic diagram and photograph of this accessory are shown in **Figure 2.10**. The beam from IR source is directed by mirrors M_1 and M_2 and focused on mirror M_3 . By changing the angle of mirror M_3 , light can be directed to various areas of the first ellipsoid, E_1 . This ellipsoid reflected light to the sample and then reflected light from the sample is collected by the second ellipsoid, E_2 and then redirects it to mirror M_4 . Mirror M_4 directs this beam to mirror M_5 and M_6 and, finally, to the detector. The angle of incidence can be changed from approximate 85 to 5 degree by rotating the mirror M_3 to sweep the beam on E_1 from left to right. One advantage, which is very important for this research, is using this accessory without requiring realignment of the sample when the angle of incidence is changed.

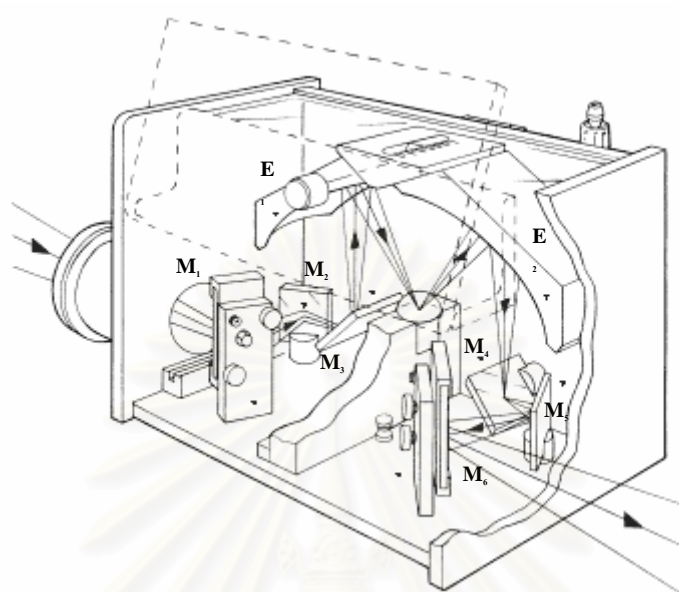


Figure 2.10 The Seagull™ Variable Angle Reflection Attachment.

2.3.3.4 ATR Spectral Intensity

If no any energy loss excepts absorption by sample, ATR spectral intensity is given by:

$$A(\theta, \nu) = 1 - R(\theta, \nu), \quad (2.5)$$

where $A(\theta, \nu)$ is absorptance and $R(\theta, \nu)$ is reflectance. Absorptance in ATR can be expressed in terms of experimental parameters and material characteristics by the following expression:

$$A_p^-(\theta, \nu) = \frac{4\pi\nu}{n_0 \cos \theta} \int_0^\infty n_1(\nu) k_1(\nu) \langle E_z^2(\theta, \nu) \rangle dz, \quad (2.6)$$

where \bar{p} is degree of polarization of the incident beam, $\langle E_z^2(\theta, \nu) \rangle$ is mean square electric field (MSEF) at depth z , $n_1(\nu)$ is refractive index of sample, $k_1(\nu)$ is absorption index of sample, and n_0 is refractive index of IRE, respectively.

The strength of MSEF is strongest at the IRE/sample interface, and exponentially decreases as a function of depth. It should be noted that MSEF is a function of experimental conditions and material characteristics. The MSEF at the interface with p-, s-, non-polarized radiation is given, respectively, by

$$\langle E_{p,z=0}^2(\theta, \nu) \rangle_{k=0} = \langle E_x^2(\theta, \nu) \rangle_{k=0} + \langle E_z^2(\theta, \nu) \rangle_{k=0} \quad (2.7)$$

$$\langle E_{s,z=0}^2(\theta, \nu) \rangle_{k=0} = \langle E_y^2(\theta, \nu) \rangle_{k=0} \quad (2.8)$$

$$\langle E_{non,z=0}^2(\theta, \nu) \rangle_{k=0} = \frac{\langle E_x^2(\theta, \nu) \rangle_{k=0} + \langle E_y^2(\theta, \nu) \rangle_{k=0} + \langle E_z^2(\theta, \nu) \rangle_{k=0}}{2} \quad (2.9)$$

where $\langle E_x^2(\theta, \nu) \rangle_{k=0}$, $\langle E_y^2(\theta, \nu) \rangle_{k=0}$, and $\langle E_z^2(\theta, \nu) \rangle_{k=0}$ are electric field of x, y, and z axis, which can be calculated by the following expressions.

$$\langle E_x^2(\theta, \nu) \rangle_{k=0} = \frac{4 \cos^2 \theta \sin^2 \theta - (n_1(\nu)/n_0)^2}{\left[1 - (n_1(\nu)/n_0)^2\right] \left\{ \left[1 + (n_1(\nu)/n_0)^2\right] \sin^2 \theta - (n_1(\nu)/n_0)^2 \right\}} \quad (2.10)$$

$$\langle E_y^2(\theta, \nu) \rangle_{k=0} = \frac{4 \cos^2 \theta}{1 - (n_1(\nu)/n_0)^2} \quad (2.11)$$

$$\langle E_z^2(\theta, \nu) \rangle_{k=0} = \frac{4 \cos^2 \theta \sin^2 \theta}{\left[1 - (n_1(\nu)/n_0)^2\right] \left\{ \left[1 + (n_1(\nu)/n_0)^2\right] \sin^2 \theta - (n_1(\nu)/n_0)^2 \right\}} \quad (2.12)$$

Figure 2.11 shows the relationship between MSEF and depth at various conditions. It can be concluded that strength and decay characteristic of the MSEF are dependent on material characteristic and experimental conditions.

Under a non-absorbing condition (i.e., $k_l(\nu) = 0$). The MSEF can be calculated if the refractive index of material is known. Under this condition, the MSEF is given a special name as the mean square evanescent field (MSEvF). Under a small absorption condition, the MSEF is closed to MSEvF. ATR intensity in absorbance unit is given in terms of experimental conditions and material characteristics as follow:

$$A_p^-(\theta, \nu) = \frac{4\pi\nu}{\ln(10)n_0 \cos \theta} \int_0^\infty n_1(\nu)k_1(\nu) \left\langle E_{z_p}^2(\theta, \nu) \right\rangle_{k=0} dz \quad (2.13)$$

After integration of Equation 5, the resulted equation is given by,

$$A_p^-(\theta, \nu) = \frac{4\pi\nu}{\ln(10)n_0 \cos \theta} n_1(\nu)k_1(\nu) \left\langle E_{z_p}^2(\theta, \nu) \right\rangle_{k=0} \frac{dp}{2} \quad (2.14)$$

Equation 2.8 shows that spectral intensity in absorbance unit is related to experimental conditions (i.e., angle of incidence) and material characteristics. It should be noted that **Equation 2.8** is only applicable small absorption because it is derived based on the MSEvF. However, this expression is the most convenient form for expressing relationship between spectral intensity and material characteristic (i.e., concentration).

2.3.3.5. Penetration Depth (d_p)

The penetration depth $d_p(\theta, \nu)$ is defined as the depth at which the electric field strength decays to 1/e of the strength at the interface. Penetration depth is given by:

$$d_p = \frac{1}{2\pi\nu n_0 (\sin^2 \theta - (n_1/n_0)^2)^{1/2}} \quad (2.15)$$

The penetration depth is a function of experimental conditions and material characteristics. Example of penetration depth at various experimental conditions and material characteristics are shown in **Figure 2.11**

สถาบันวิทยบริการ
จุฬาลงกรณ์มหาวิทยาลัย

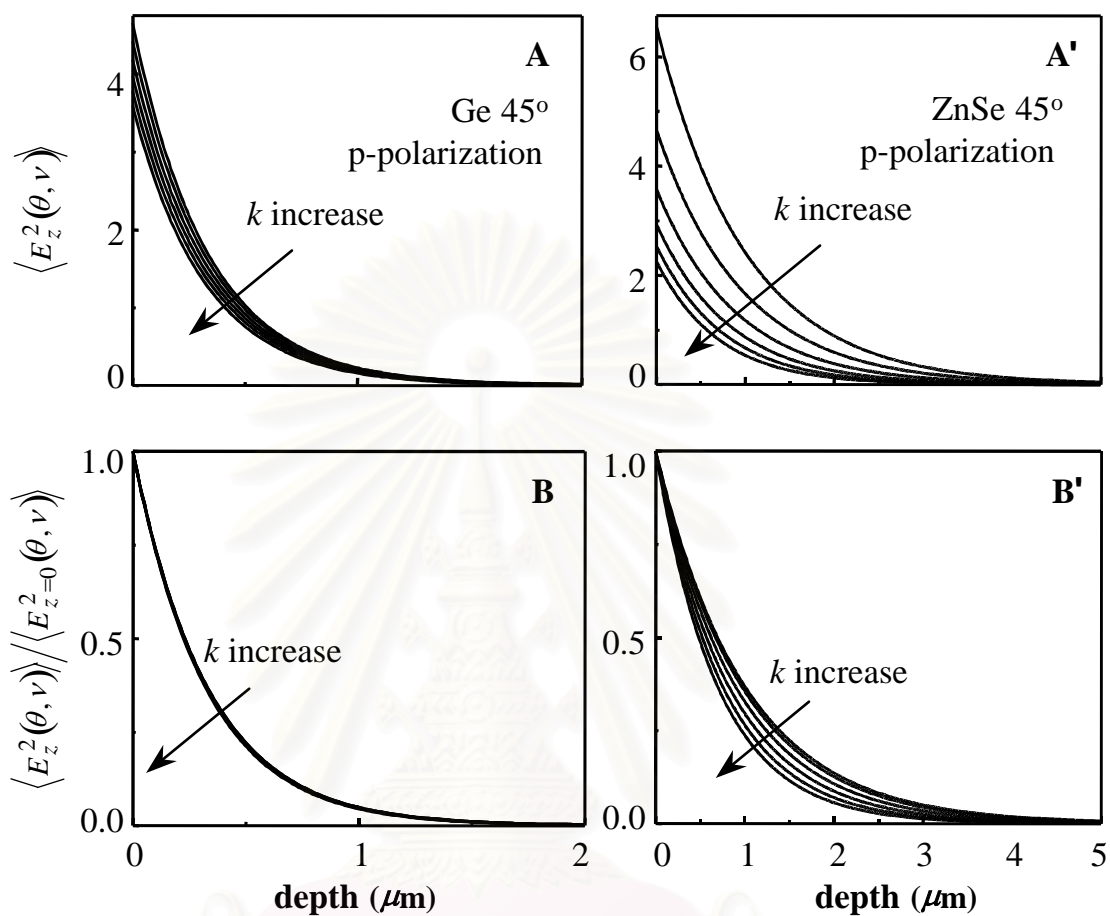


Figure 2.11 Relationship between MSEF and depth at various experimental conditions (A, A') and its decay characteristic (B, B'). The simulation parameters are $n_0 = 4.0$ for Ge IRE, $n_0 = 2.40$ for ZnSe IRE, $\nu = 1,000 \text{ cm}^{-1}$, $n_1(\nu) = 1.5$, and $k_1(\nu) = 0.0, 0.1, 0.2, 0.3, 0.4$, and 0.5 .

2.3.3.6 Optical Contact in ATR Experiment

2.3.3.6.1 Problem of Sample Contact in ATR Measurement

To obtain a good ATR spectrum, very good contact between the sample and IRE is required because ATR FT-IR is a surface characterization technique. Optical contact or perfect contact always achieves between liquid sample and IRE. Unfortunately, solid samples rarely have a good contact with an IRE although their surface is obviously flat. This is due to defect on the surface, and surface irregularity of the sample. The use of applied pressure can improve the sample contact but still no optical contact is obtained. Moreover, excessive pressure may lead to rapid deterioration of the prism because materials of which ATR prism is made are not very strong.

In order to compare two spectra quantitatively, the samples must have perfect contact or having the same thickness of air gap. Considering two spectra of the same sample, if air gaps of two spectra are not equal, spectra intensity is not equal. The reason is the unequal of electric field decay in two media, which have different refractive indices. Electric field decays faster in the media, which have a greater different in refractive index from prism. Then, electric field decays faster in air ($n_0=1$) than in the sample ($n_1=1.5$ for organic sample). An air gap makes electric field decay faster. Absolutely, less electric field reaches the sample and smaller absorbance is observed.

If two systems with different air gap are considered, their spectra are quantitatively incomparable by using the peak ratio. The reason is the nonlinear relationship between d_p and frequency in ATR technique (**Figure 2.12**). As a result, the characteristic peaks at high frequency from the high air gap spectrum may disappear, while those at low frequency still remain.

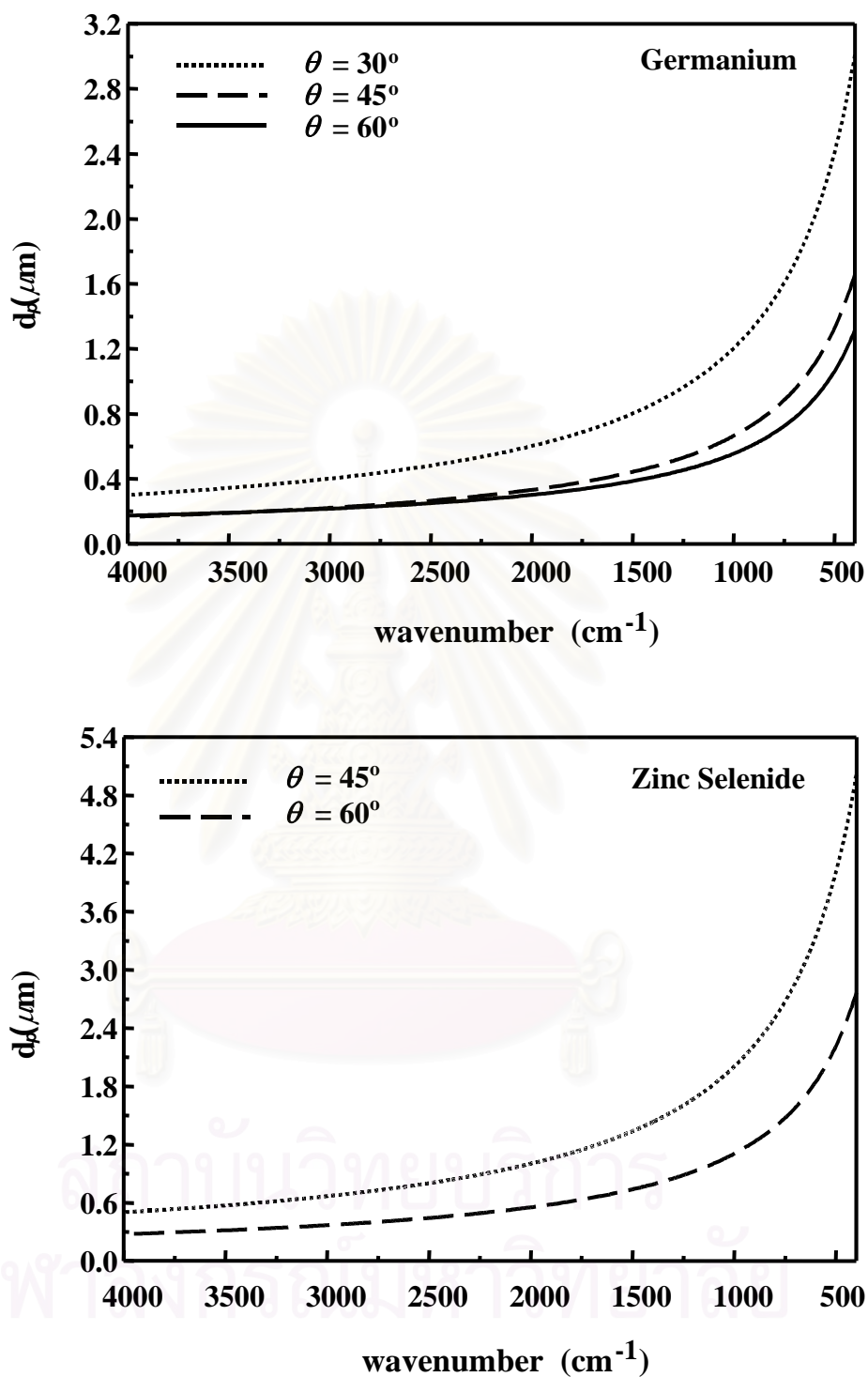


Figure 2.12 Penetration depth at various experimental conditions for germanium and zinc selenide IRE.

In this research, by using Seagull™, the angle of incidence of infrared beam can be changed without any sample realignment. If a perfect contact is achieved, the spectra from different sample could be compared.

Nowadays, there is not any applicable technique for perfect contact between solid sample and prism. Several techniques were proposed to improve contact such as the uses of fluid pressure⁴⁴, diamond prism^{45,46}, and liquid buffer layer.⁴⁷ Unfortunately, there is no any applicable and effective techniques.⁴⁷ Thus, mechanical pressure is remained the widely used technique to improve contact. Contact between prism and sample can be determined as follow.⁴⁸⁻⁵¹

$$A_p(45^\circ, \nu) = 2A_s(45^\circ, \nu), \quad (2.16)$$

where A_p is absorbance of p-polarized spectrum and A_s is absorbance of s-polarized spectrum.

For optical contact system, A_p/A_s ratio at 45-degree angle of incidence is equal to 2. The closer the value to 2, the better the contact between sample and IRE.

สถาบันวิทยบริการ
จุฬาลงกรณ์มหาวิทยาลัย

2.3.4 Depth Profiling by ATR FT-IR Spectroscopy

Attenuated total reflection Fourier transform infrared (ATR FT-IR) spectroscopy is one of the most useful and well-known techniques for the characterization of polymeric films. After the first introduction of ATR technique, a number of applications including surface characterization and depth profiling of polymeric films were developed. In the past two decades, there were many publications on ATR FT-IR spectroscopy, including depth profiling by multiple angle ATR FT-IR spectroscopy.¹¹⁻¹⁴

ATR FT-IR can be used as a depth profiling technique since condition varying, such as angle of incidence, led to changing of penetration depth of electric field into the substrate. Therefore, by changing of angle of incidence, the information of different depth was achieved. The composition at any depth can be represented by several methods, such as concentration, volume fraction, and complex refractive index of the material. Among these methods, the technique used to represent the film composition at any depth by nk value is the simplest compared to that by concentration, volume fraction, and complex refractive index of pure component. The difficulty of using the last three methods is absorption coefficient or extinction coefficient profiles have to be accurately assumed. This requirement limits the applicability of those methods since it is difficult to predict the accurate profile. On the other hand, nk value technique does not require dealing with any difficulty mentioned above including complex refractive index.

For a nonabsorbing medium, the refractive index n is given simply as the ratio of the velocity of light in vacuum c to that in the sample v , $n=c/v$. For isotropic substance, n of any point is equal. Absorption index k is the constant expressed absorptivity of sample at a specific wavenumber. High k means that light is highly absorbed by sample, cause to high absorption intensity. K at any wavenumber depends on absorption properties of sample. It should be noted that k , at a specific wavenumber, at any point of isotropic substrate is constant.

For an isotropic substrate at a specific wavenumber, n and k are constant. Therefore, nk value is constant. From this point, nk value was able to identify whether the sample is isotropy. If nk value of sample is not constant, the sample is anisotropic material. In this research, nk values at various depths of crosslinked chitosan film were investigated. Thus, depth dependent property of crosslinked chitosan film could be examined. The peaks used for nk calculation are the peaks at 1654 and 1564 cm^{-1} , which are characteristic peaks of imine and amine group respectively. Both functional groups are directly related to crosslinking reaction.

The depth dependent composition of a polymeric film can arise from variations in processing conditions such as diffusion, surface treatment, and temperature. As a result of film treatments, film compositions are not constant, especially in the depth direction. In this research, depth dependent properties of chitosan films both before and after crosslinked were investigated by ATR FT-IR spectroscopy. After spectra manipulation and mathematical operation, a depth dependent property was determined by mean of nk value.



สถาบันวิทยบริการ
จุฬาลงกรณ์มหาวิทยาลัย

CHAPTER 3

EXPERIMENT

3.1 Preparation of Crosslinked Chitosan Films

3.1.1 Materials and Equipment

1. Chitosan

The chitosan flakes used in this research was the product of Seafresh Chitosan (Lab) Co., Ltd. The specification is given in **Table 3.1**.

2. Glutaraldehyde solution 25% analytical grade from Riedel-de Haen
3. Glacial acetic acid analytical grade from J.T.Baker
4. Sodium hydroxide pellet analytical grade from Akzo Nobel
5. Acrylic plate (10x10x1cm³)
6. One side crosslinking Set
7. Oven
8. Electric balance
9. Glassware

สถาบันวิทยบริการ
จุฬาลงกรณ์มหาวิทยาลัย

Table 3.1 Specification of chitosan

Item	Specification	Chitosan
1. Appearance	Yellowish	Yellowish
2. Particle size	Mesh No.18	Mesh No.18
3. Ash content	Less than 1.0%	0.15%
4. Moisture content	Less than 10.0%	9.0%
5. Deacetylation	95% Minimum	95%
6. Solution (1% acetic acid)		
Insoluble (%)	Less than 1.0%	0.4%
Viscosity	500 cps Minimum	648 cps
7. Heavy metal	Less than 20 ppm	0 ppm
8. Microbial content		
Total plate count	Less than 1,000 cfu. /g.	380
Yeast&mold	Less than 100 cfu. /g.	40
E.coli	Nil	Nil
Salmonella	Nil	Nil

3.1.2 Preparation of One-Side Crosslinked Chitosan Films

1. Chitosan flakes were used as received. Dissolving chitosan flakes (3 g.) in of 1% acetic acid solution (197 g.) at room temperature. The mixture was left to dissolve overnight.
2. Chitosan solution (14.0 g.) was poured onto leveled clean acrylic molds and allowed to dry under ambient condition for 3 days.
3. Dried chitosan films were fixed on acrylic mold, leaving no air gap between molds and films.

4. One side neutralized by pouring 7g/l NaOH solution (40 ml.) into a fixed area and left for 120 minutes.
5. Washed by distilled water for several times to remove excess NaOH solution.
6. One-side-crosslinked chitosan films were prepared by pipetting 28.5 ml. of 1370 ppm glutaraldehyde solution onto the fixed area and left for 0, 10, 100, 1000 minutes.
7. Washed by distilled water for several times to remove excess glutaraldehyde solution.
8. The films were then baked in 60°C oven for 5 hours.
9. The films were allowed to cool down and kept in desiccator.

3.1.3 FT-IR Spectrometer Conditions

Bruker vector 33 FT-IR spectrometer

Experimental setup

Resolution 4.0 cm^{-1}

Number of scans 32

Result spectrum Absorbance

Optic parameters

Source setting Globar (MIR)

Detector setting DIGS

Beam splitter setting KBr

3.1.4 Spectra Acquisitions

1. Uncrosslinked chitosan film, approximately 10 microns thickness, was placed in transmission sample holder.
2. Transmission spectra were acquired using non-polarized radiation.
3. Transmission spectra of 10, 100, and 1000 minutes crosslinked chitosan films were acquired.

3.2 Accuracy of Programs Used for nk Calculation

3.2.1 Spectra Simulation Conditions

1. $n_0 = 4.0$
2. $n_1 = 1.4$
3. Non-polarization
4. Angle of incidence = 37, 39, 41, 43, 45, 47, 49 degree
5. Started wavenumber = 4000
6. Ended wavenumber = 400
7. Spectral resolution = 2
8. Peak position = 1640, 1560
9. Half width at half height = 10
10. Absorption index = 0.02 and 0.5

3.3 nk Value of Isotropic Substrate

3.3.1 Materials and Equipment

1. Nujol
2. Variable angle single attenuated total reflection accessories from Harrick (**Seagull**TM)
3. Ge hemispherical IRE
4. Bruker Vector 33 FT-IR spectrometer

3.3.2 Spectra Acquisitions

1. Nujol was spread as a liquid film over Ge IRE.
2. An ATR spectrum of nujol at 37-degree angle of incidence was acquired by using non-polarized radiation.

3. Series of spectra were acquired by varying angle of incident to 39, 41, 43, 45, 47, and 49 degree.

3.4 *nk* Value of Chitosan Film

3.4.1 Materials and Equipment

1. Chitosan film
2. Angle-variable single attenuated total reflection accessories
3. Ge hemisphere IRE from Spectra Tech.
4. Bruker Vector 33 FT-IR spectrometer
5. IR polarizer

3.4.2 Spectra Acquisitions

1. Air-side of chitosan film was placed against Ge IRE while pressure was applied on to the sample.
2. ATR spectra of the system at 37-degree angle of incident were acquired repeatedly every 5 minutes until there is no any difference between the last 2 spectra.
3. Additional ATR spectra were acquired by varying angle of incidence to 39, 41, 43, 45, 47, and 49-degree.
4. With polarizer, ATR spectra at 45-degrees and p-polarization were acquired.
5. Placing mold-side of chitosan film against Ge IRE and following the four steps above. Series of spectra of mold-side were acquired.

3.5 *nk* Value of Crosslinked Chitosan Films

3.5.1 Materials and Equipment

1. Crosslinked chitosan films
2. Nujol
3. Angle-variable single attenuated total reflection accessories
4. Ge hemisphere IRE from Spectra Tech.
5. Bruker Vector 33 FT-IR spectrometer
6. IR polarizer

3.5.2 Spectra Acquisitions

1. Air-side of 10 minutes crosslinked chitosan film was placed against Ge IRE with pressure applied.
2. ATR spectra of the system at 37-degree angle of incident were acquired repeatedly every 5 minutes until there is no any difference between the last 2 spectra.
3. By using non-polarized radiation, series of ATR spectra were acquired by varying angle of incidence to 39, 41, 43, 45, 47, and 49-degree.
4. With polarizer, ATR spectra at 45-degree s and p-polarization were acquired.
5. By placing mold-side of chitosan film against Ge IRE and following the four steps above, series of spectra of mold-side were acquired.
6. By changing 10 minutes crosslinked chitosan film to 100 and 1000 minutes crosslinked chitosan films and following the five steps above, series of spectra of both air and mold side of 100 and 1000 minutes crosslinked chitosan films were acquired.

CHAPTER 4

RESULTS AND DISCUSSION

4.1 Preparation of Crosslinked Chitosan Films

Chitosan films with approximately 10 μm thickness with one-side crosslinking were investigated. After crosslinking process, IR spectra of crosslinked films were acquired using transmission technique. The characteristic peaks were those at 1655 and 1564 cm^{-1} , which indicated C=N stretching of imine group and N-H bending of amine and acetamido group, respectively. It should be noted that before crosslinking, peak at 1655 was observed because this wavenumber was also be absorbed by C=O stretching of acetamido group. However, acetamido group was not affected by crosslinking reaction. As a result, changing of peak height at 1655 cm^{-1} was only referred to occurring of imine group from crosslinking reaction. Transmission spectra of chitosan films are shown in Figure 4.1. The films were one-side crosslinking for 0, 10, 100, and 1000 minutes. In this figure, the peak height at 1564 cm^{-1} was equalized for easier comparison. A peak shift from 1582 to 1564 cm^{-1} was observed after crosslinking. As a result, the spectra of 0-minute crosslinking time could not be compared with others. By comparing the spectra of 10, 100 and 1000 minutes crosslinking time, peak height at 1655 cm^{-1} increased when crosslinking time was increased. This clear observation indicates that crosslinking reaction has taken place and the extent of reaction is increased as a function of time. Moreover, absorption at 1720 cm^{-1} , belong to C=O stretching of aldehyde group, was not observed from spectra 0 minute and 10 minutes but was observed from spectra 100 minutes and 1000 minutes. This indicated that there was no aldehyde group in the film crosslinked for 10 minutes but in the films crosslinked for 100 and 1000 minutes. The increment of peak height at 1720 cm^{-1} by time could also be concluded that if crosslinking time was increased, aldehyde group in the films was increased. It should be noted that aldehyde group in crosslinked film could come from

crosslinking reaction as proposed by Muzzarelli¹, formation of glutaraldehyde oligomer and unreacted aldehyde groups.

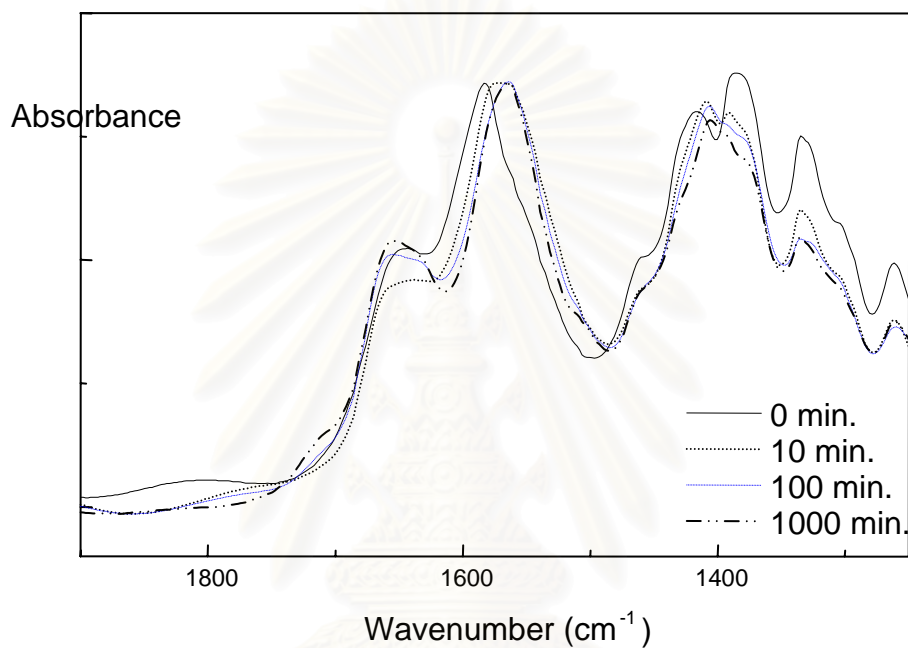


Figure 4.1 Transmission spectra of chitosan films crosslinked with various crosslinking times.

สถาบันวิทยบริการ
จุฬาลงกรณ์มหาวิทยาลัย

4.2 Accuracy of Programs Used for nk value Calculation

In this research, nk values were used to determine the depth dependent properties of crosslinked chitosan film. Since nk value was calculated from complex expression, mathematical programs were used to calculate nk value. The programs used for nk value calculation in this research were written. Proving the accuracy of programs was performed by using them to calculate nk value of the spectrum with known nk value. (i.e., those were simulated spectra). Simulated spectra are spectra simulated from spectra simulation programs by input all of necessary terms for spectra simulation in to simulation programs, including n , k , wavenumber, angles of incidence. In order to simulate the closed to real spectrum, the value of each necessary term used for spectra simulation were the same as the actual experimental. The n and k values used for spectra simulation were 1.43 and 0.1, as a result, nk values of all simulated spectra were 0.143. Absorbance of simulated spectra is shown in **Figure 4.2**. Absorbance of spectrum with a smaller angle of incidence is greater than that of a larger angle of incidence. This is due to greater electric field strength at a smaller angle of incidence.

The nk values of simulated spectra calculated from Figure 4.2 are shown in **Figure 4.4**. The consistencies of nk values at about 0.028 implies that the programs used for calculating nk value were accurate. Moreover, the linear of nk value in each wavenumber indicated that the condition be used for spectra provided the small absorption spectra. Thus, these conditions were believed to provide the small absorption spectra in the real sample system. Theoretically, if the spectra had small absorption, linear relationship between nk and angles of incidence of isotropic substrate were acquired. On the other hand, nonlinear relationship between nk values and angles of incidence of isotropic substrate might be observed in a high absorption system. The conditions led to increase of absorption consist of high wavenumber, low angle of incidence high k , etc. **Figure 4.3 and 4.5** are spectra simulated from high absorption condition and relationship between nk values and angles of incidence of high absorption system. Although the input nk values were constant, one could observe that nonlinearly between nk values and angles of incidence were presented.

It should be noted that changing of nk values could be observed easier if linear relationship between nk values and angles of incidence was presented.



สถาบันวิทยบริการ
จุฬาลงกรณ์มหาวิทยาลัย

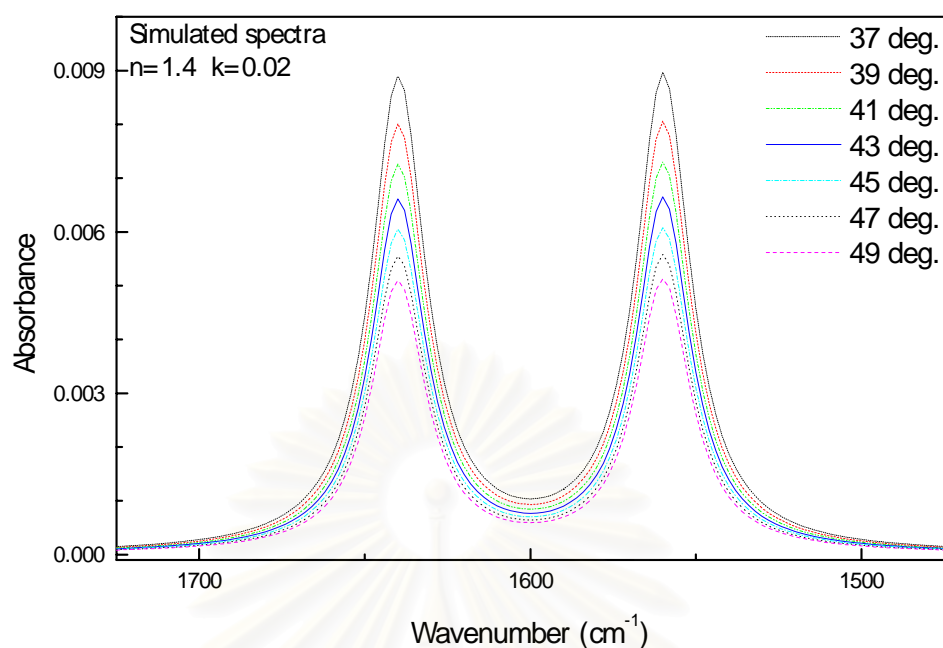


Figure 4.2 Simulated ATR spectra of film at various angles of incidence. The simulation parameters are $n_{\text{film}}=1.4$, $n_{\text{IRE}}=4.0$, $k_{\text{film}}=0.02$, angles of incidence=37, 39, 41, 43, 45, 47, and 49 degree.

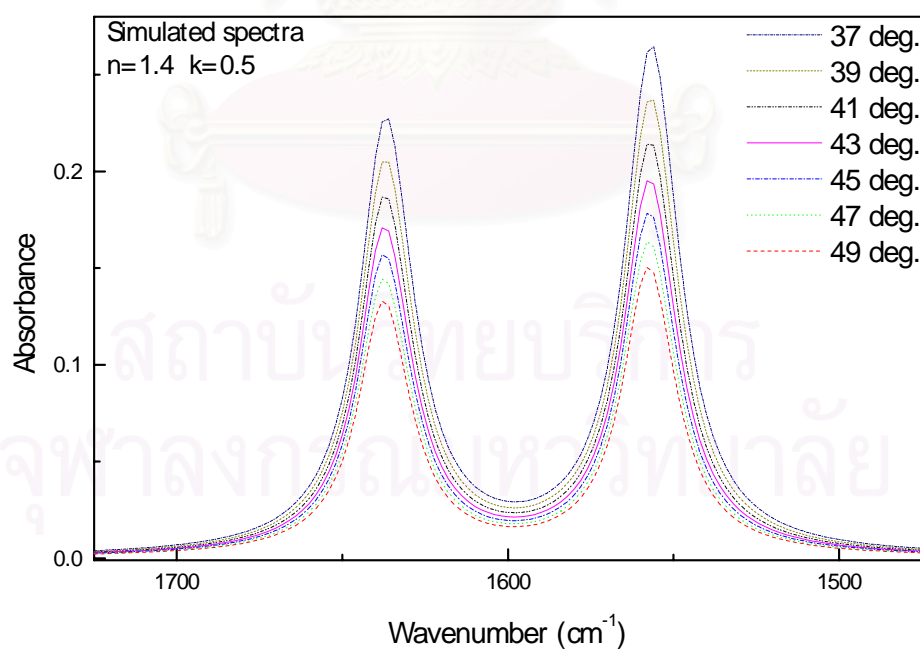


Figure 4.3 Simulated ATR spectra of film at various angles of incidence. The simulation parameters are $n_{\text{film}}=1.4$, $n_{\text{IRE}}=4.0$, $k_{\text{film}}=0.5$, angles of incidence=37, 39, 41, 43, 45, 47, and 49 degree.

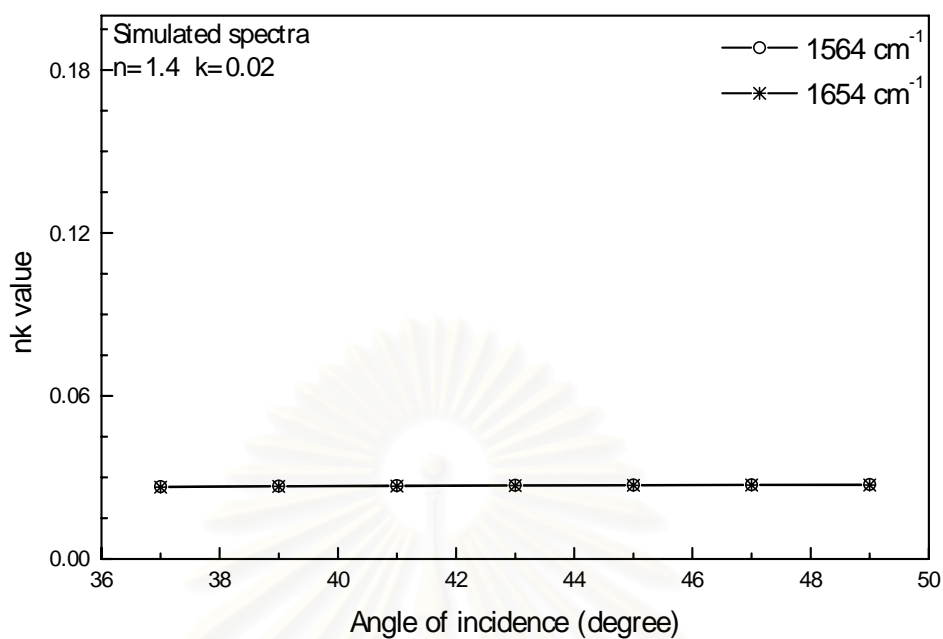


Figure 4.4 Relationship between angles of incidence and nk values of simulated spectra with small absorption. The spectra used for calculation were those from **Figure 4.2**.

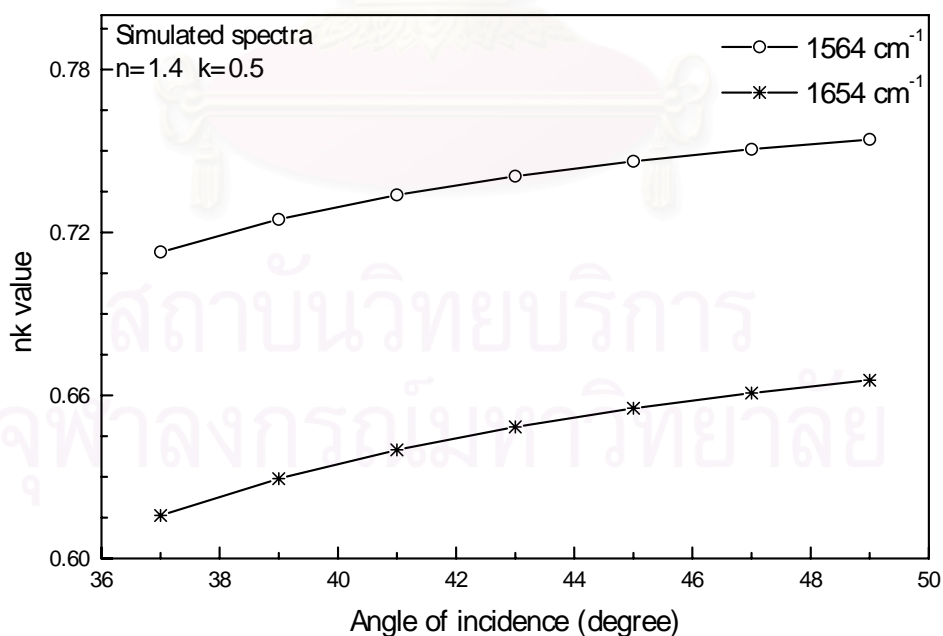


Figure 4.5 Relationship between angles of incidence and nk values of simulated spectra with high absorption. The spectra used for calculation were those from **Figure 4.3**.

4.3 nk Value of Isotropic Substrate

Before using nk value calculation programs with chitosan films, the programs were evaluated again with series of real spectra of the sample, which had not depth dependent characteristics. As described in 4.2, the relationship between nk values and angles of incidence of isotropic sample with small absorption condition must be linear. The isotropic sample was nujol, a non-volatile and viscous liquid consists of low molecular weight alkane. It should be noted that nujol has optical contact with the IRE. Spectra of nujol were acquired by angle variable ATR attachment. Peak height at 1458 and 1376 cm^{-1} was employed for nk values calculation. Complete spectrum of nujol and peaks used for nk calculation are shown in Figure 4.6. The spectra of nujol at various angles of incidence are shown in **Figure 4.7**. Relationship between angles of incidence and nk values is shown in **Figure 4.8**. A linear relationship between nk values and angles of incidence are observed.

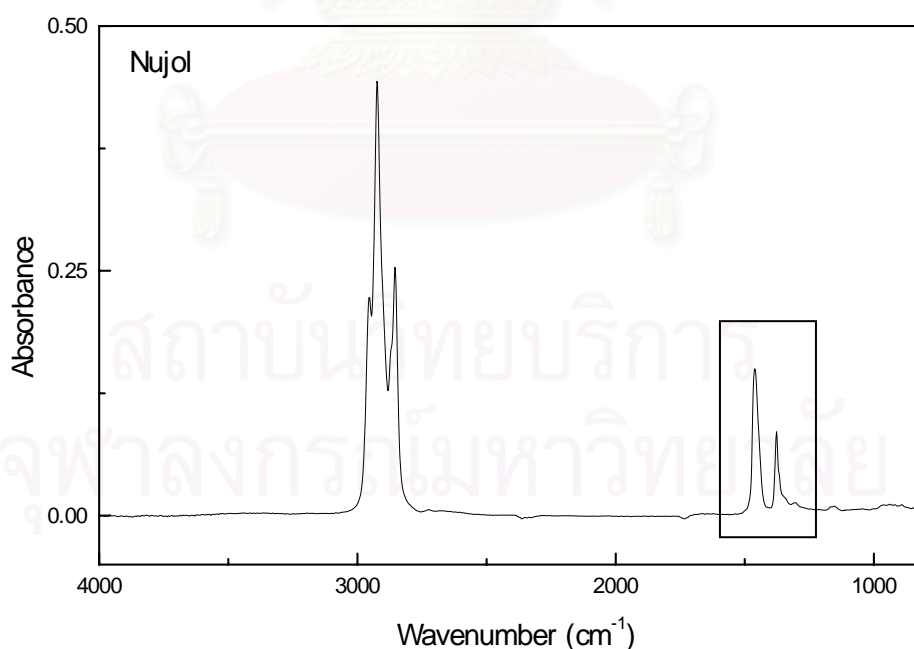


Figure 4.6 ATR spectra of nujol acquired via Ge IRE at 45-degree angle of incidence.

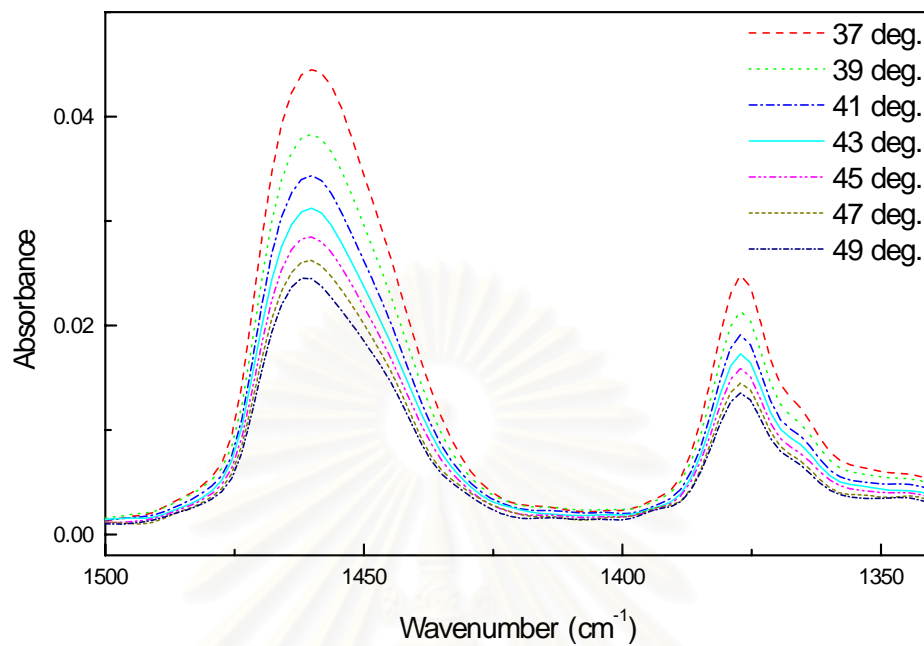


Figure 4.7 ATR spectra of nujol at 37, 39, 41, 43, 45, 47, and 49 degree angles of incidence.

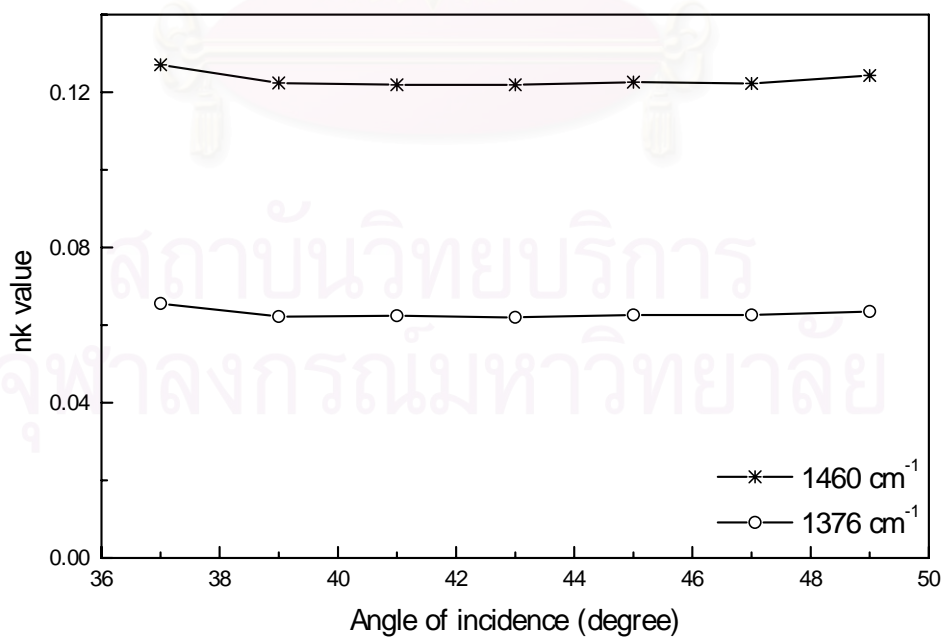


Figure 4.8 Relationship between angles of incidence and nk values of nujol. The spectra used for calculation were those from **Figure 4.7**.

4.4 *nk* Value of Chitosan Film

The *nk* values of both side of uncrosslinked chitosan film were determined. The objectives are to determine whether or not uncrosslinked chitosan film has depth dependent property. The *nk* values of uncrosslinked film will be used for comparing with those of crosslinked films. When the sample has small absorption, *nk* values of the sample without depth dependent property is constant.

ATR technique was used for spectral acquisition. By varying the angles of incidence, two series of spectra were acquired, those from air-side and those from mold-side of chitosan film. The spectra are shown in **Figure 4.9 and 4.10**, respectively. Absorption peak at 1655 and 1564 cm^{-1} were used for *nk* values calculation. In **Figure 4.11 and 4.12**, respectively, relationships between angles of incidence and *nk* values of air side and mold side are shown. From **Figure 4.11**, the constant of *nk* values at various angles of incidence was observed at both 1655 and 1564 cm^{-1} . It could be concluded that there was not depth dependent property of the mold-side of uncrosslinked chitosan film. From **Figure 4.12**, which *nk* values of air-side of chitosan film were shown, the inconstant of *nk* values at different angles of incidence was observed at 1655 and 1564 cm^{-1} . This observation indicated that there were depth dependent properties of the air-side chitosan film. It should be noted that the depth dependent characteristic of chitosan films observed were less than 0.6 μm from film surface. Penetration depth of each wavenumber are shown in **Table 4.1**

Table 4.1 Penetration depth at various angles of incidence of the wavenumber used to calculate nk values.

Angles of incidence (degree)	Penetration depth (micron)	
	At 1655 wn.	At 1564 wn.
37	0.5154	0.5419
39	0.4801	0.5047
41	0.4507	0.4738
43	0.4259	0.4477
45	0.4047	0.4255
47	0.3864	0.4062
49	0.3704	0.3894

From the above observation, it can be concluded that

1. At the air-sided, there was no depth dependent property of the chitosan film.
2. At mold-sided, there was depth dependent property of the chitosan film.

The result of this part shown that there was difference between air sided and mold sided of uncrosslinked chitosan film prepared from solvent casting technique. This observation corresponded with those observed by other researchers.⁵²

Morphology of both air and mold surface of solvent cast chitosan film was observed via scanning electron microscope. They reported that morphology of both surfaces of chitosan films was much different.

สถาบันวิทยบริการ
จุฬาลงกรณ์มหาวิทยาลัย

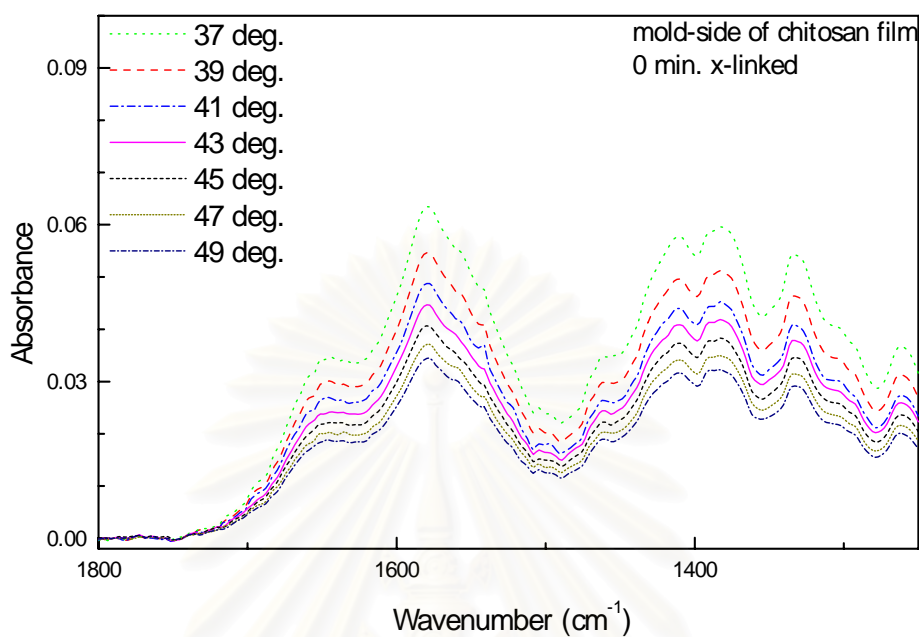


Figure 4.9 ATR spectra of uncrosslinked chitosan film (mold-side) acquired via Ge IRE at 37, 39, 41, 43, 45, 47, and 49 degree angles of incidence.

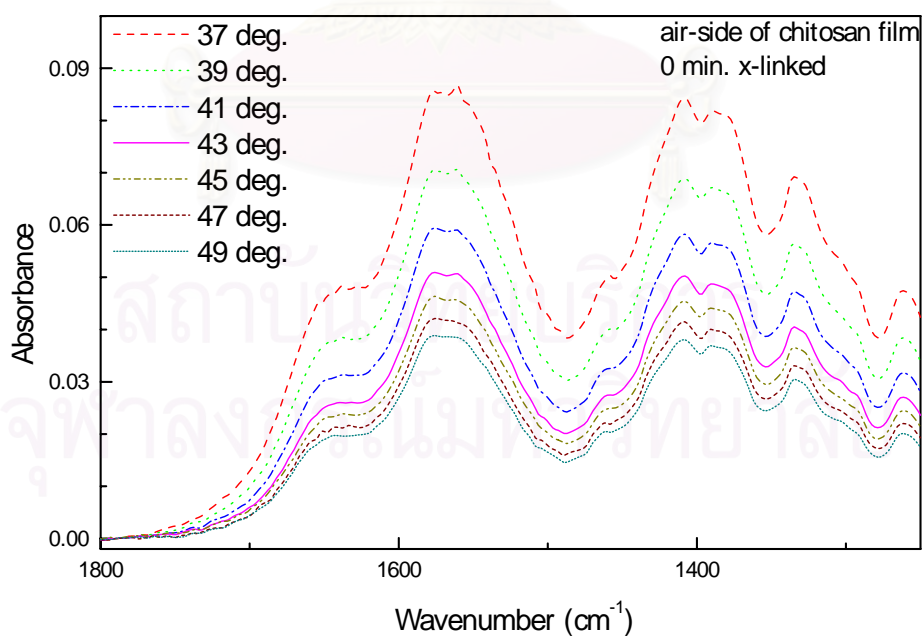


Figure 4.10 ATR spectra of uncrosslinked chitosan film (air-side) acquired via Ge IRE at 37, 39, 41, 43, 45, 47, and 49 degree angles of incidence.

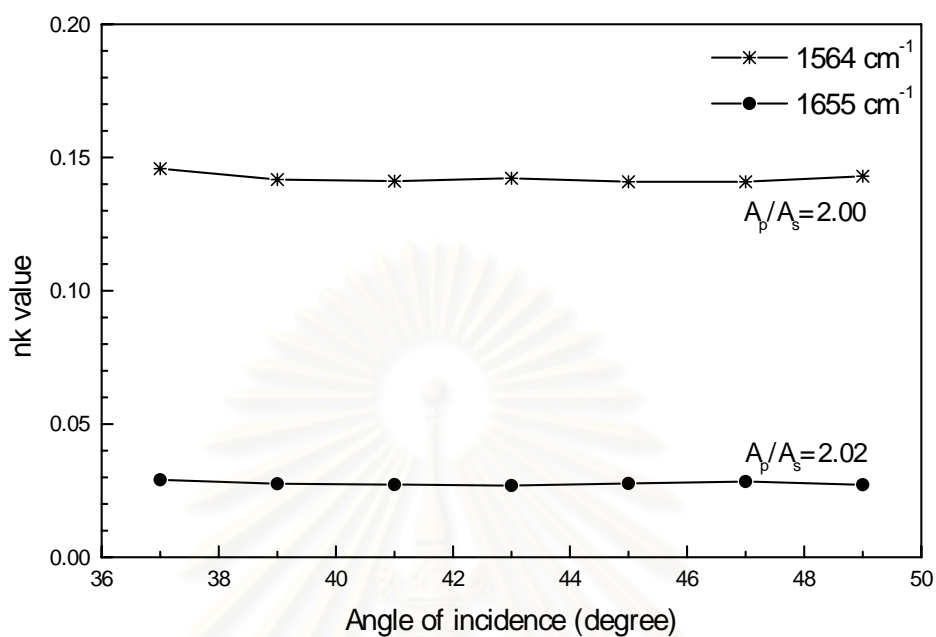


Figure 4.11 Relationship between angles of incidence and nk values of uncrosslinked chitosan film (mold-side). The spectra used for calculation were those from **Figure 4.9**.

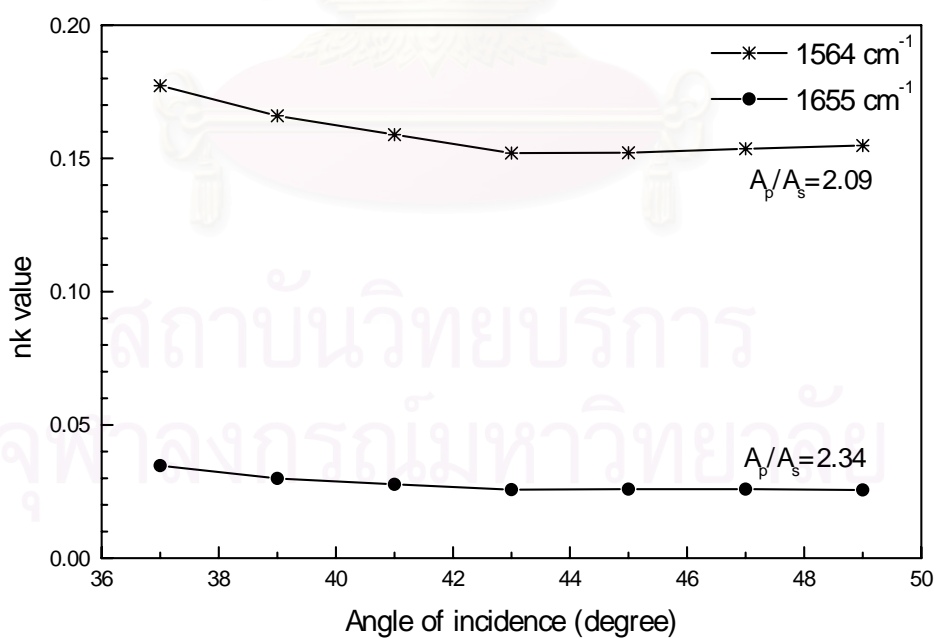


Figure 4.12 Relationship between angles of incidence and nk values of uncrosslinked chitosan film (air-side). The spectra used for calculation were those from **Figure 4.10**.

4.5 nk Value of Crosslinked Chitosan Films

The nk values of both sides of crosslinked chitosan films were determined. The main purpose was to observe whether or not crosslinked chitosan films obtained by heterogeneous reaction have depth dependent properties. Chitosan films were air-side crosslinked for 10, 100, and 1000 minutes. ATR IR spectra were acquired from both sides of the films. The series of spectra and peaks used for calculation are shown in **Figure 4.13 to 4.18**.

Figure 4.19, 4.21, and 4.23 show relationship between nk values and angles of incidence of mold sided of chitosan films crosslinked for 10, 100, and 1000 minutes, respectively. There was small variation of nk values in each series. However, the insignificant of changing of nk value and the random changing indicate that there was not depth dependent property in the observed sample.

Figure 4.20, 4.22, and 4.24 are relationship between nk values and angles of incidence of air-side of chitosan films crosslinked for 10, 100, and 1000 minutes, respectively. Focusing on A_p/A_s ratio of each series, A_p/A_s ratio of 10 minutes series was closed to 2, where as A_p/A_s ratio of 100 and 1000 minutes series were much lower than 2. Moreover, A_p/A_s ratio was observed to decrease by increasing of crosslinking time. The far from two of A_p/A_s ratio of 100 and 1000 minutes series mean that the contact between chitosan films and prism of this two series was far from optical contact, results to the low reliability of these two series. The decrement of A_p/A_s ratio by increasing of crosslinking time could be explained that more crosslinking time resulted to more crosslinking reaction of chitosan films, led to more rigidity of chitosan films and resulted to decreasing of contact. The far from two of A_p/A_s ratio of 100 and 1000 minutes series led to unreliable of nk values.

The unchanged of nk value graph observed between **Figure 4.12** and **Figure 4.16** indicated that depth dependent properties of air-side of chitosan film, crosslinked for 10 minutes were not different from the depth dependent properties of air-side of uncrosslinked chitosan film.

Figure 4.25 and 4.26 show the spectra of mold-side of chitosan films crosslinked with different crosslinking times acquired via ATR FT-IR at 39 and 41 degree angles of incidence, respectively. The increment of peak height at 1654 and 1710 cm^{-1} by crosslinking time indicated that crosslinking reaction was also taken place at the mold-side of crosslinked chitosan film. Moreover, crosslinking reaction increased with crosslinking time.

Figure 4.27 and 4.28 show the spectra of air-side of chitosan crosslinked with different crosslinking times acquired via ATR FT-IR at 39 and 41 degree angles of incidence, respectively. There was increment of peak height at 1654 cm^{-1} when crosslinking time increased from 10 to 100 min., whereas there was no increment of peak height at the same peak when crosslinking time increased from 100 to 1000 min. This observation indicated that there was no increment of imine linkage after 100 minutes crosslinking time.

Figure 4.29 4.30 and 4.31 show the spectra both mold-side and air-side of crosslinked chitosan films crosslinked for 10, 100, and 1000 minutes, respectively. The angle of incidence used for spectra acquisition was 39 degree. The peak height at 1654 and 1710 cm^{-1} of the air-side of the film was higher than those of the mold-side. This observation indicated that the crosslinking density of the air-side was greater than those of the mold side. As a result, it was concluded that there were depth dependent properties of the crosslinked films.

From overall observation, the conclusions can be drawn.

1. Crosslinking reaction took place and increased by crosslinking time from 10-1000 minutes.
2. The *nk* calculation programs could be used accurately with the simulated and real spectra.
3. In this research, depth dependent properties of chitosan films were not observed at the mold side but were observed at air-side. At air-side, composition of amine and acetamido group at deeper layer was greater than the shallower layer. It should be noted that the observed depth was 0-0.5 μm in range.

4. A_p/A_s ratio of mold side was not changed by crosslinking time. Thus, the increasing of crosslinking time did not affect the contact property of mold side surface.
5. A_p/A_s ratio of air-side surface was decreased by increasing crosslinking time. It could be concluded that increasing of crosslinking time reduced the contact property of crosslinked side surface.
6. Crosslinking reaction was also taken place at the mold-side of crosslinked chitosan film. Moreover, crosslinking reaction increases by increase crosslinking time.
7. At the air-side, there was no increment of imine linkage after 100 minutes crosslinking time.
8. There were depth dependent properties of the films crosslinked in this research.

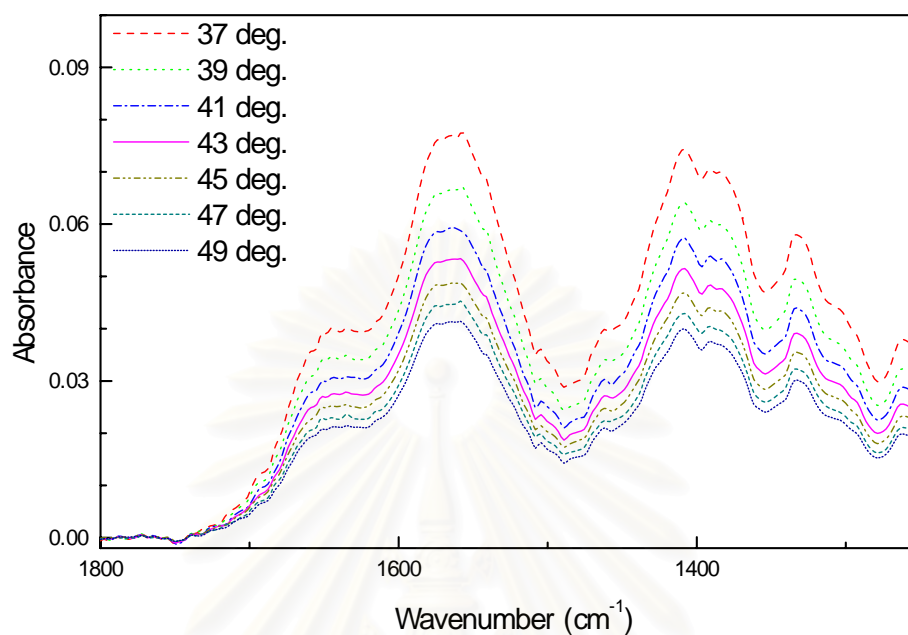


Figure 4.13 ATR spectra of 10 minutes crosslinked chitosan film (mold-side) acquired via Ge IRE at 37, 39, 41, 43, 45, 47, and 49 degree angles of incidence.

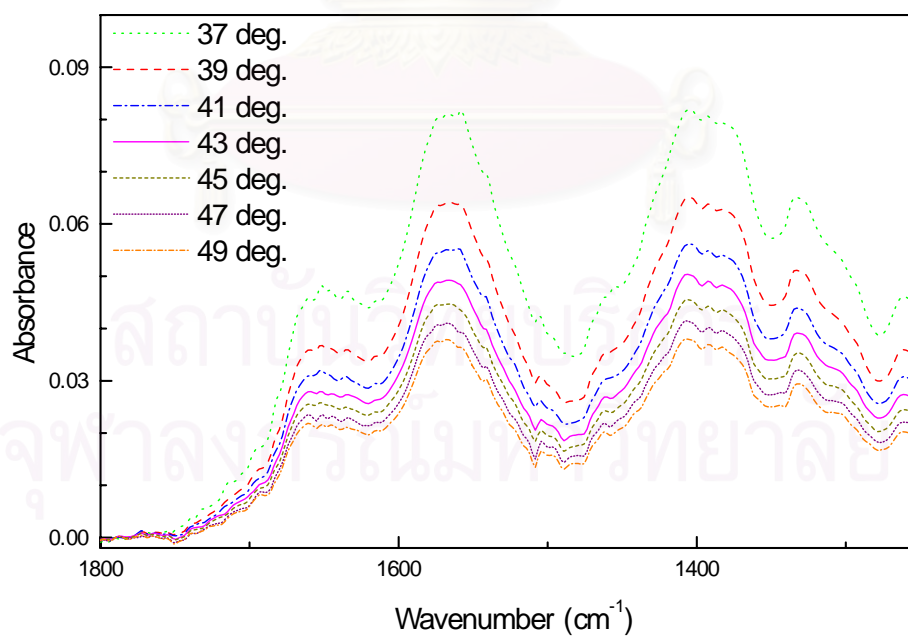


Figure 4.14 ATR spectra of 10 minutes crosslinked chitosan film (air-side) acquired via Ge IRE at 37, 39, 41, 43, 45, 47, and 49 degree angles of incidence.

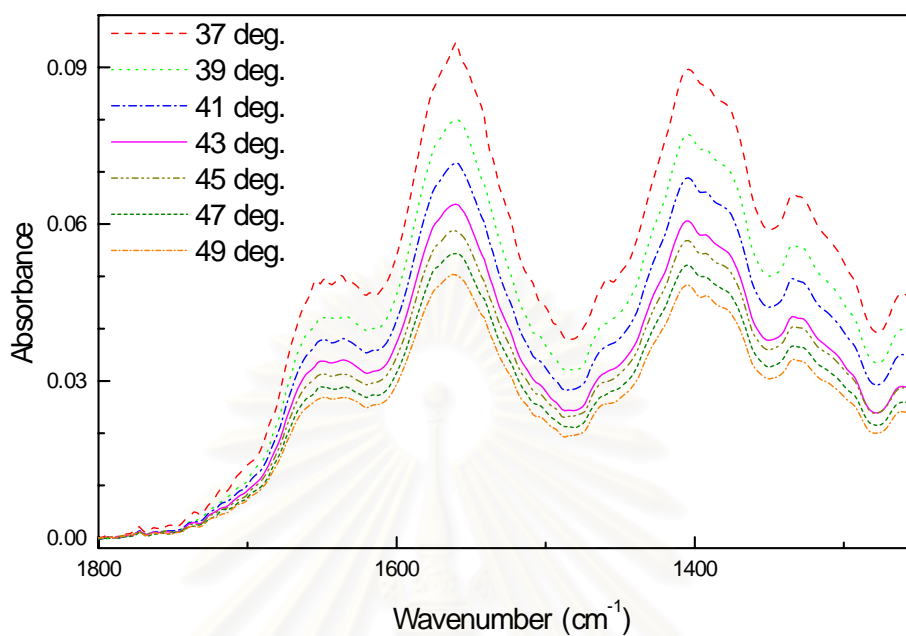


Figure 4.15 ATR spectra of 100 minutes crosslinked chitosan film (mold-side) acquired via Ge IRE at 37, 39, 41, 43, 45, 47, and 49 degree angles of incidence.

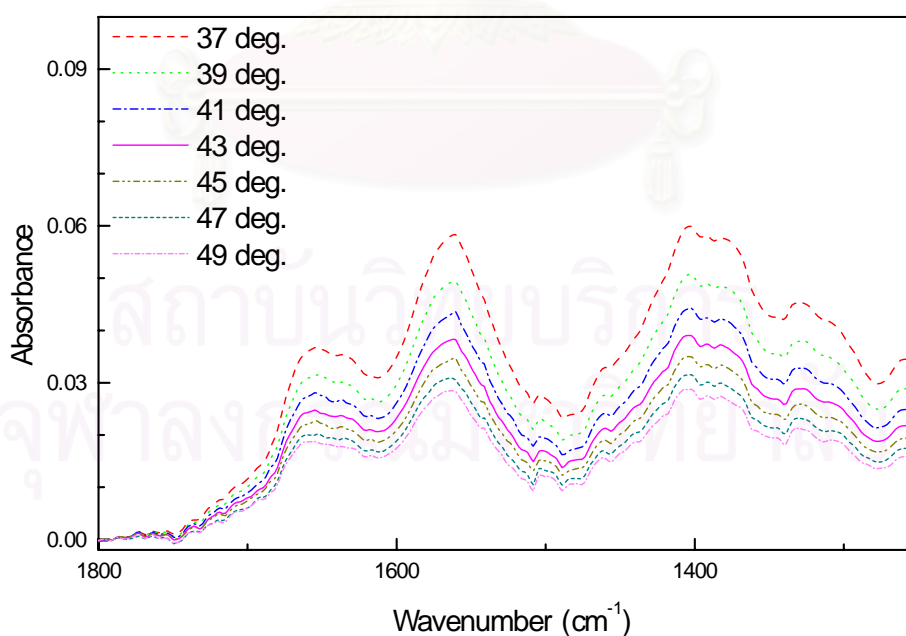


Figure 4.16 ATR spectra of 100 minutes crosslinked chitosan film (air-side) acquired via Ge IRE at 37, 39, 41, 43, 45, 47, and 49 degree angles of incidence.

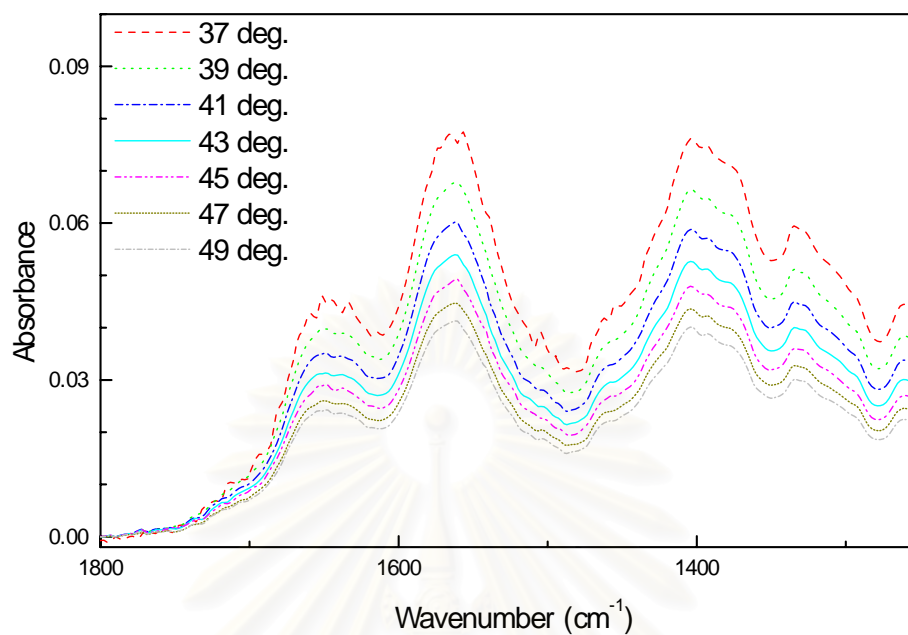


Figure 4.17 ATR spectra of 1000 minutes crosslinked chitosan film (mold-side) acquired via Ge IRE at 37, 39, 41, 43, 45, 47, and 49 degree angles of incidence.

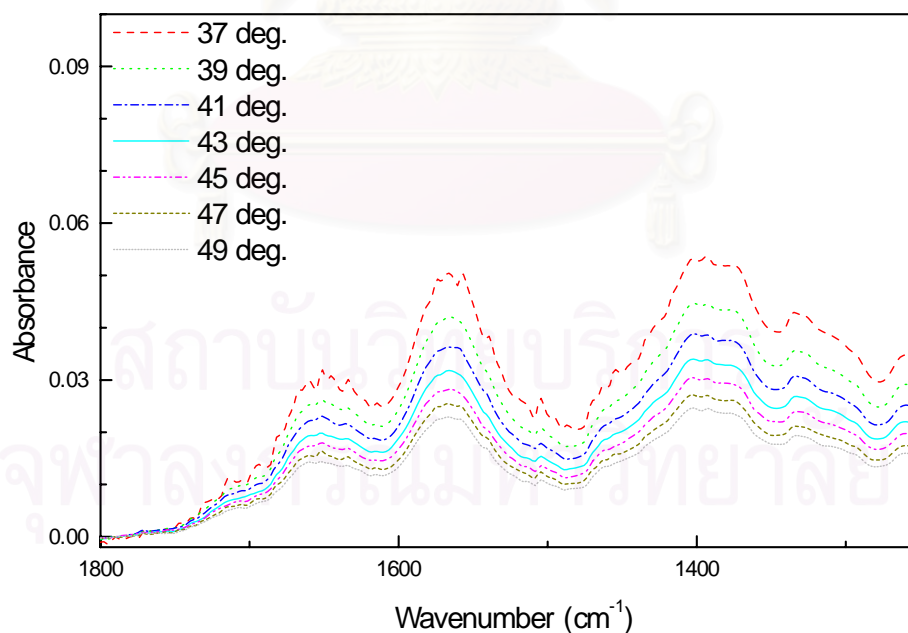


Figure 4.18 ATR spectra of 1000 minutes crosslinked chitosan film (air-side) acquired via Ge IRE at 37, 39, 41, 43, 45, 47, and 49 degree angles of incidence.

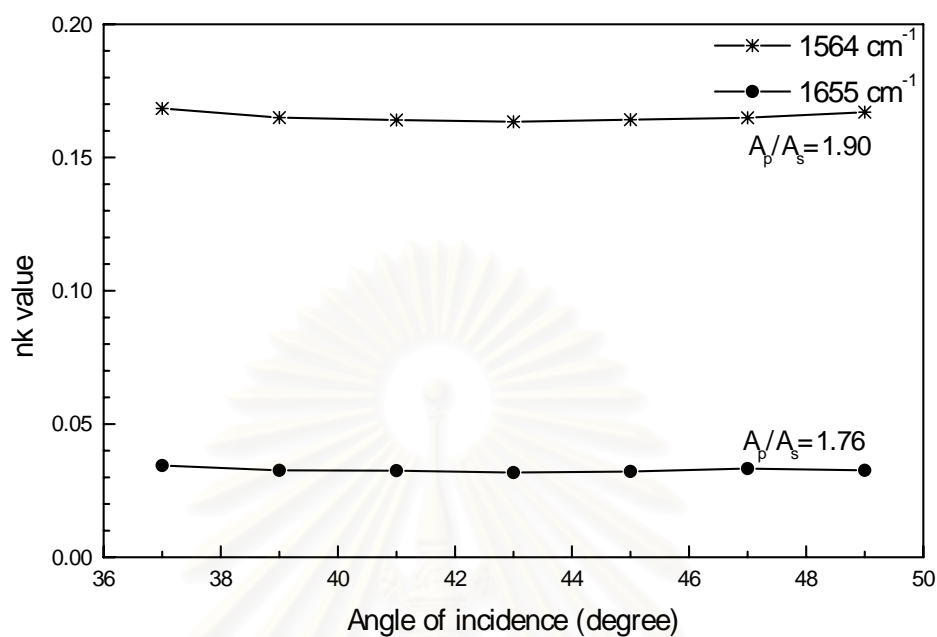


Figure 4.19 Relationship between angles of incidence and nk values of 10 minutes crosslinked chitosan film (mold-side). The spectra used for calculation were those from **Figure 4.13**.

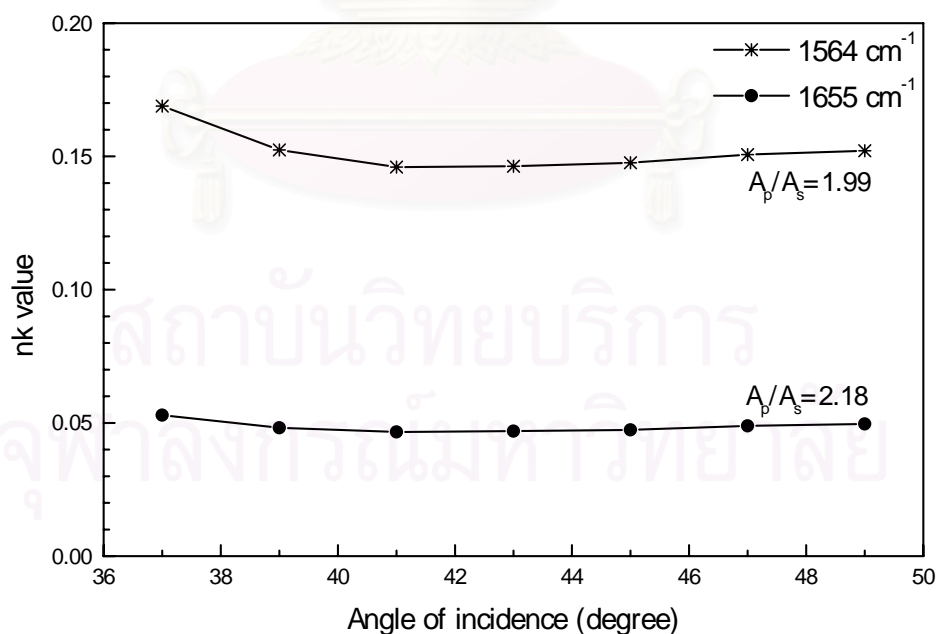


Figure 4.20 Relationship between angles of incidence and nk values of 10 minutes crosslinked chitosan film (air-side). The spectra used for calculation were those from **Figure 4.14**.

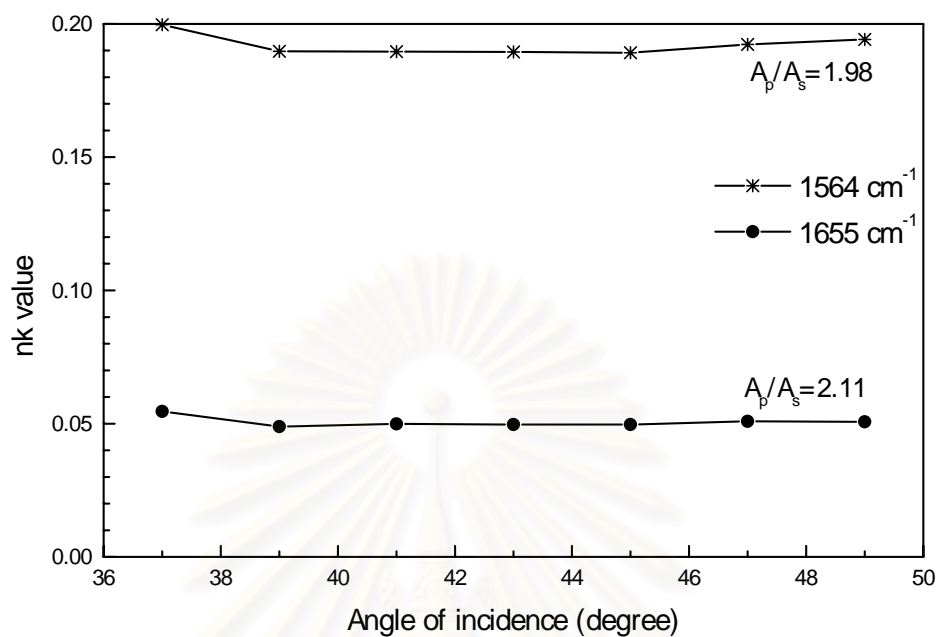


Figure 4.21 Relationship between angles of incidence and nk values of 100 minutes crosslinked chitosan film (mold-side). The spectra used for calculation were those from **Figure 4.15**.

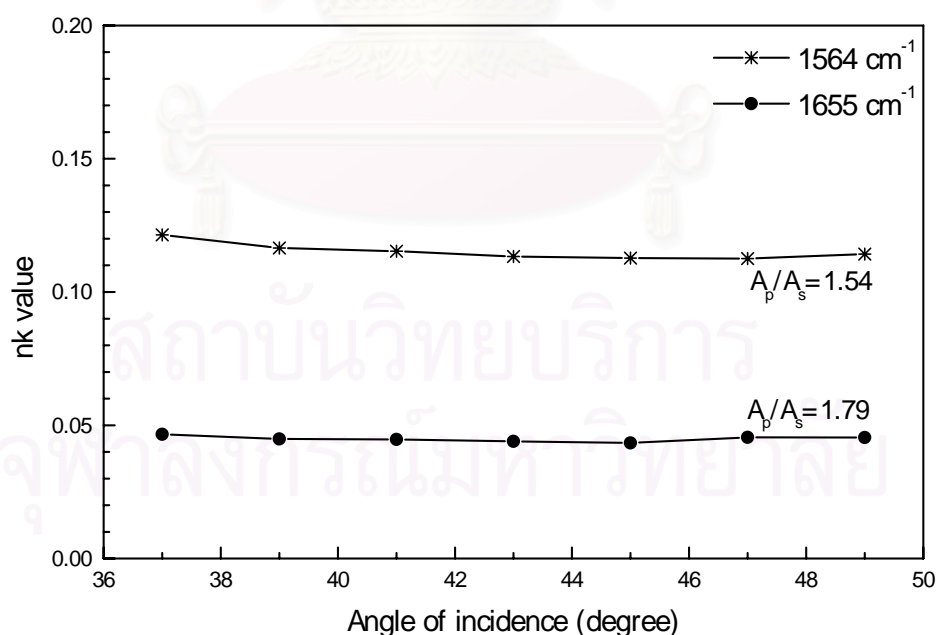


Figure 4.22 Relationship between angles of incidence and nk values of 100 minutes crosslinked chitosan film (air-side). The spectra used for calculation were those from **Figure 4.16**.

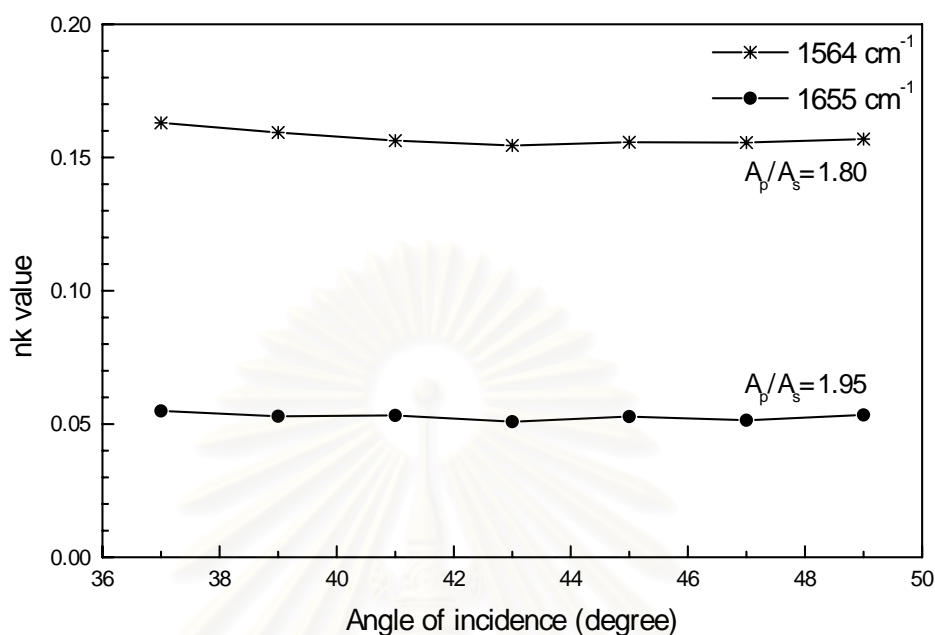


Figure 4.23 Relationship between angles of incidence and nk values of 1000 minutes crosslinked chitosan film (mold-side). The spectra used for calculation were those from **Figure 4.17**.

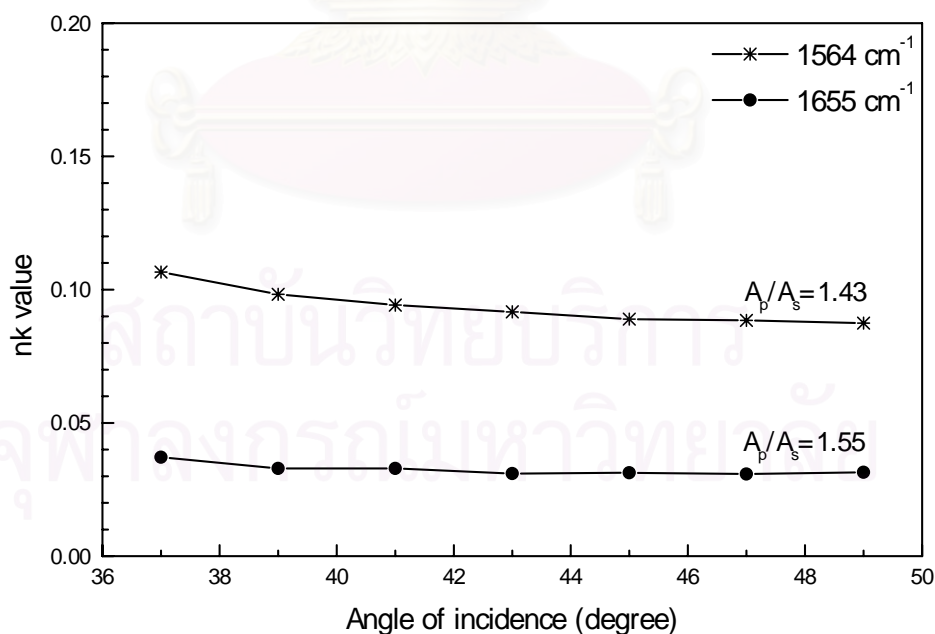


Figure 4.24 Relationship between angles of incidence and nk values of 1000 minutes crosslinked chitosan film (air-side). The spectra used for calculation were those from **Figure 4.18**.

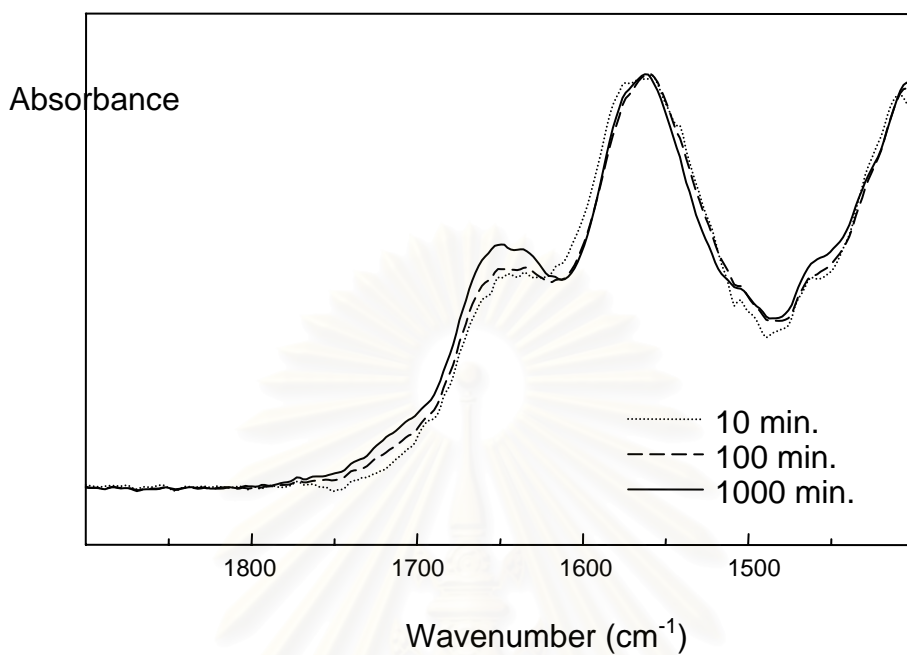


Figure 4.25 ATR spectra of chitosan films (mold-side) crosslinked with various times acquired via Ge IRE at 39 degree angle of incidence.

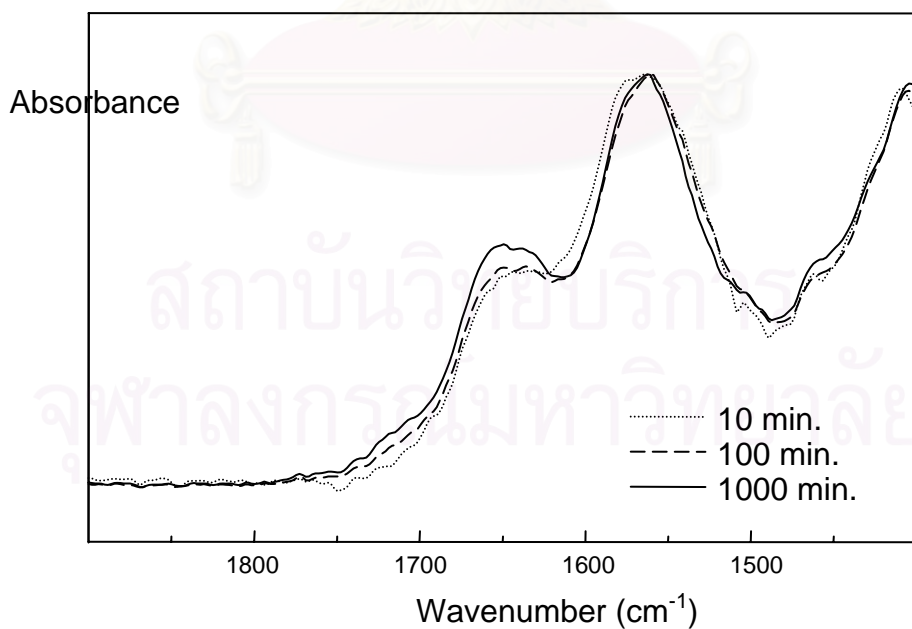


Figure 4.26 ATR spectra of chitosan films (mold-side) crosslinked with various times acquired via Ge IRE at 41 degree angle of incidence.

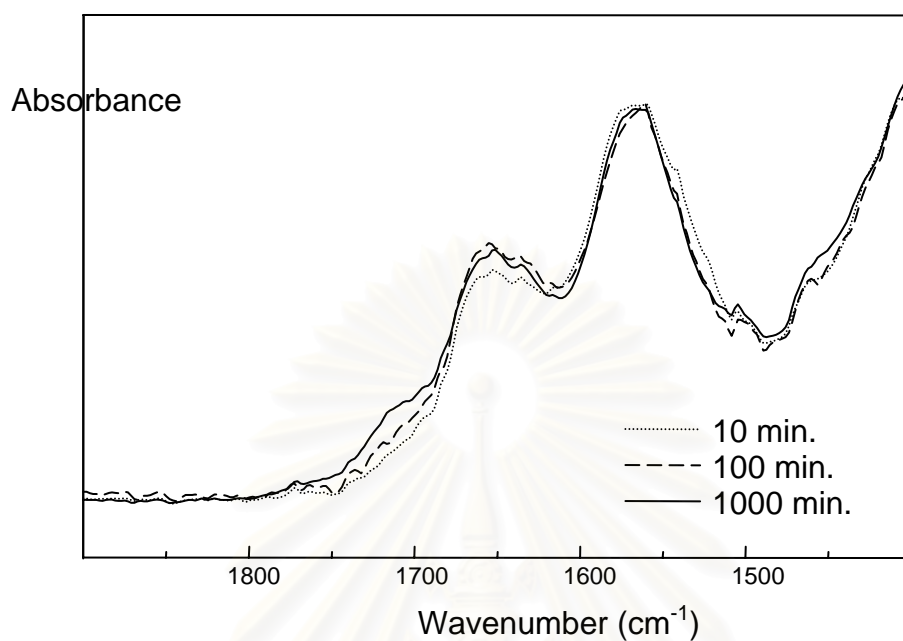


Figure 4.27 ATR spectra of chitosan films (air-side) crosslinked with various times acquired via Ge IRE at 39 degree angle of incidence.

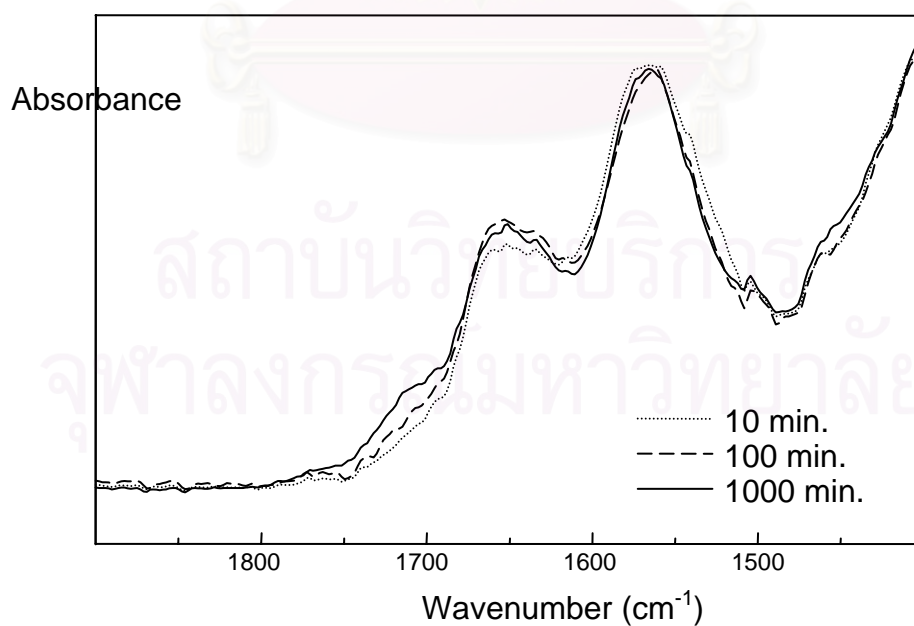


Figure 4.28 ATR spectra of chitosan films (air-side) crosslinked with various times acquired via Ge IRE at 41 degree angle of incidence.

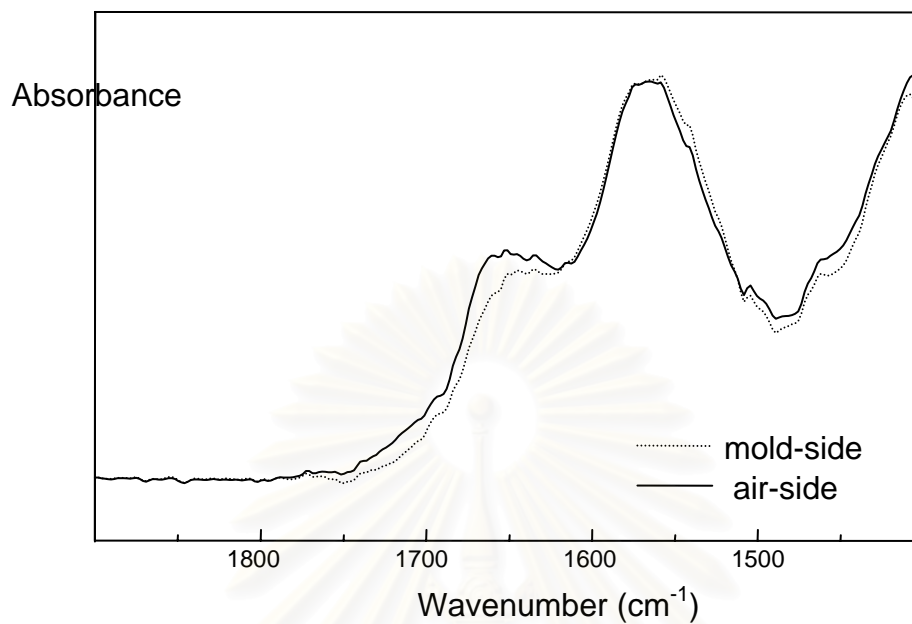


Figure 4.29 ATR spectra of 10 minutes crosslinked chitosan film acquired via Ge IRE at 39 degree angle of incidence.

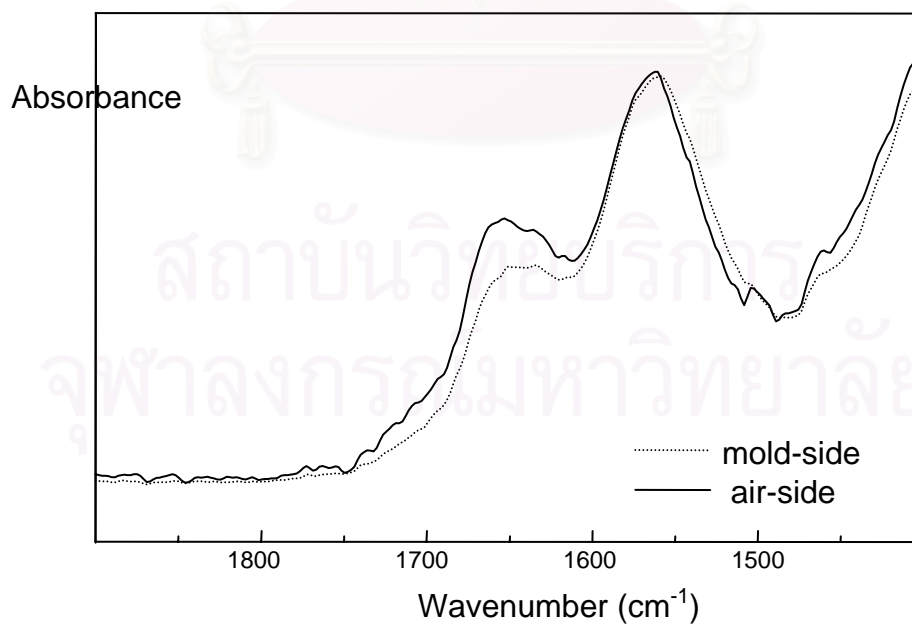


Figure 4.30 ATR spectra of 100 minutes crosslinked chitosan film acquired via Ge IRE at 39 degree angle of incidence.

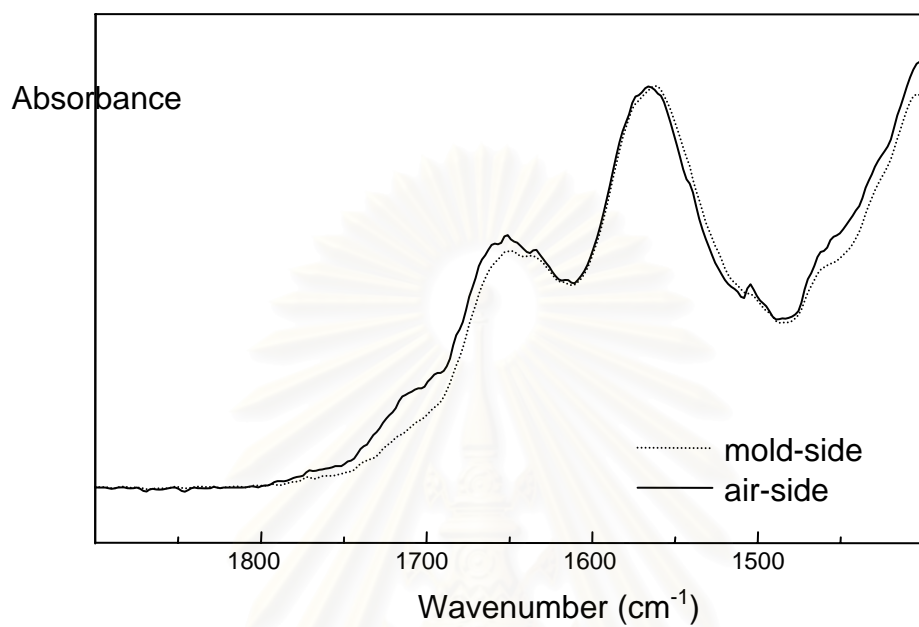


Figure 4.31 ATR spectra of 1000 minutes crosslinked chitosan film acquired via Ge IRE at 39 degree angle of incidence.

สถาบันวิทยบริการ
จุฬาลงกรณ์มหาวิทยาลัย

CHAPTER 5

CONCLUSION

From the results presented in this research, it was concluded that:

- 1 Crosslinking reaction occurred and increased with crosslinking time.
- 2 There was difference of acetamido and amine groups composition between mold-side and air-side of the film.
- 3 Software programs established to calculate nk value could be used accurately with both simulated and real spectra.
- 4 There was depth dependent crosslinking density of glutaraldehyde crosslinked chitosan film by heterogeneous procedure. The crosslinking density was highest at the surface, which contacted crosslinking solution and decreased as a function of depth.
- 5 Crosslinking reaction occurred up to 10 μm depth from crosslinked surface of the film.

สถาบันวิทยบริการ
จุฬาลงกรณ์มหาวิทยาลัย

REFERENCES

1. Tual, C.; Espuche, E.; Escoubes M.; and Domard, A. Journal of Polymer Science 38 (2000): 1521-1529.
2. Andrady, A.L.; and Xu, P. Elastic behavior of chitosan films. Journal of Polymer Science: Part B: Polymer Physics 35(1997): 517-521.
3. Denkbasi, E.B. and Odabasi, M. Chitosan microspheres and sponges: preparation and characterization. Journal of Applied Polymer Science 76(2000): 1637-1643.
4. Matsuyama, H.; Kitamura, Y.; and Naramura, Y. Diffusion permeability of ionic solutes in charged chitosan membrane. Journal of Applied Polymer Science 72(1999): 397-404.
5. Thacharodi, D.; and Rao, K.P. Development and in vitro evaluation of chitosan-based transdermal drug delivery systems for the controlled delivery of propranolol hydrochloride. Biomaterials 16(1995): 145-148.
6. López, C.R.; and Bodmeier, R. Mechanical, water uptake and permeability properties of crosslinked chitosan glutamate and alginate films. Journal of Controlled Release 44(1997): 215-225.
7. Musale, D.A.; and Kumar, A. Effects of surface crosslinking on sieving characteristics of chitosan/poly(acrylonitrile) composite nanofiltration membranes. Separation and Purification Technology 21(1995): 27-38.
8. Musale, D.A.; and Kumar, A. Solvent and pH resistance of surface crosslinked chitosan/poly(acrylonitrile) composite nanofiltration membranes. Journal of Applied Polymer Science 77(2000): 1782-1793.
9. Knaul, J.Z.; Hudson, S.M.; and Creber, K.A. Crosslinking of chitosan fibers with dialdehydes : proposal of new reaction mechanism. Journal of Polymer Science: Part B: Polymer Physics 37(1999): 1079-1094.
10. Thacharodi, D.; and Rao, K.P. Release of nifedipine through crosslinked chitosan membranes. International Journal of Pharmaceutics 96(1993): 33-39.

11. Ekgasit, S.; and Ishida, H. Application of a new quantitative optical depth profiling technique for the diffusion of polymers. Applied Spectroscopy 51(1997): 461-465.
12. Pihlajamäki, A.; Väisänen, P.; and Nyström, M. Characterization of clean and fouled polymeric ultrafiltration membranes by fourier transform IR spectroscopy-attenuated total reflection. Colloids and Surface A: Physicochemical and Engineering Aspects 138(1998): 323-333.
13. Sung, H.W.; Huang, R.N.; Huang, L.L.; Tsai, C.C.; and Chiu, C.T. Feasibility study of a natural crosslinking reagent for biological tissue fixation. Journal of Biomedical Materials Research 42(1998): 560-567.
14. Wernke, T.M.; and Offermann, V. Depth profiling of porous silicon layers by attenuated total reflection spectroscopy. Thin Solid Films 255(1995): 181-184.
15. Martinou, A.; Kafetzopoulos, D.; and Bouriotis, V. Chitin deacetylation by enzymatic means: monitoring of deacetylation processes. Carbohydrate research 273(1995): 235-242.
16. Tsigos, I.; Martinou, A.; Kafetzopoulos, D.; and Bouriotis, V. Chitin deacetylases: new, versatile tools in biotechnology. Tibtech 18(2000): 305-312.
17. A. Tolaimate, J. Desbrières, M. Rhazia, A. Alaguic, M. Vincendon, and P. Vottero. On the influence of deacetylation process on the physicochemical characteristics of chitosan from squid chitin. Polymer 41(2000): 2463-2469.
18. Kim, C.Y.; Choi, H.M.; and Cho, H.T. Effect of deacetylation on sorption of dyes and chromium on chitin. Journal of Applied Polymer Science 63(1996): 725-736.
19. Mima, S.; Miya, M.; Iwamoto, R.; and Yoshikawa, S. Highly deacetylated chitosan and its properties. Journal of Applied Polymer Sciences 28(1983): 1909-1917.
20. Chinadit, U.; Wanichpongpan, P.; How, N.C.; Stevens, W.F.; and Chandrkrachang, S. Chemical deacetylation of shrimp chitin in different conditions.: 165-168.

21. Li, J.; Revol, J.F.; and Marchessault, R.H. Effect of degree of deacetylation of chitin on the properties of chitin crystallites. Journal of Applied Polymer Science 65(1996): 373-380.
22. Shigemasa, Y.; Matsuura, H.; Sashiwa, H.; and Saimoto, H. Evaluation of different absorbance ratios from infrared spectroscopy for analyzing the degree of deacetylation in chitin. International journal of biological macromolecules 18(1996): 237-242.
23. Duarte, M.L.; Ferreira, M.C.; Marvão, M.R.; and Rocha, J. Determination of the degree of acetylation of chitin materials by ¹³C CP/MAS NMR spectroscopy. International Journal of Biological Macromolecules 28(2001): 359–363.
24. Shigemasa, Y.; Matsuura, H.; Sashiwa, H.; and Saimoto, H. Evaluation of different absorbance ratios from infrared spectroscopy for analyzing the degree of deacetylation in chitin. International Journal of Biological Macromolecules 18(1996): 237-242
25. Palace, G.P.; and Phoebe, C.H. Quantitative determination of amino acid levels in neutral and glucosamine-containing carbohydrate polymers. Analytical Biochemistry 244(1997): 393–403.
26. Curotto, E.; and Aros, F. Quantitative determination of chitosan and the percentage of amino groups. Analytical Biochemistry 211(1993): 240-241.
27. Hiroaki, S.; et al. Determination of the degree of acetylation of chitin/chitosan by pyrolysis-gas chromatography in the presence of oxalic acid
28. Heux, L.; Brugnerotto, J.; Desbrières, J.; Versali, M.F.; and Rinaudo, M. Solid state NMR for determination of degree of acetylation of chitin and chitosan. Biomacromolecules 1(2000): 746-751.
29. Ferreira, M.C.; Duarte, M.L.; and Marvão, M.R. Determination of the degree of acetylation of chitosan by FT-IR spectroscopy: KBR discs vs. films.: 129-134.
30. กาวดี เมธะคานนท์, อศิรา เฟื่องฟูชาติ และกิ่งเกียรติ คงสุวรรณ. Chitin chitosan. (ม.ป.ท., ม.ป.ป.).
31. Ravindra, R.; Krovvidi, K.R.; and Khan, A.A. Solubility parameter of chitin and chitosan. Carbohydrate polymers 36(1998): 121-127.

32. Oungbho, K.; and Müller, B.W. Chitosan sponges as sustained release drug carriers. International Journal of Pharmaceutics 156(1997): 229-237.
33. Monteiro, O.; and Airoidi, C. Some studies of crosslinking chitosan-glutaraldehyde interaction in a homogeneous system. International Journal of Biological Macromolecules 26(1999): 119-128.
34. Cheng, G.X.; et al. Studies on dynamic behavior of water in crosslinked chitosan hydrogel. Journal of Applied Polymer Science 67(1998): 983-988.
35. Nam, S.Y.; and Lee, Y.M. (1999). Pervaporation separation of methanol/methyl t-butyl ether through chitosan composite membrane modified with surfactants. Journal of Membrane Science 157(1999): 63-71.
36. Mi, F.L.; Shyu, S.S.; Lee, S.T.; and Wong, T.B. Kinetic study of chitosan-tripolyphosphate complex reaction and acid-resistive properties of the chitosan-tripolyphosphate gel beads prepared by in-liquid curing method. Journal of Polymer Science Part B-Polymer Physics 37(1999): 1551-1564.
37. Mi, F.L.; Sung, H.W.; and Shyu, S.S. Synthesis and characterization of a novel chitosan-based network prepared using naturally occurring crosslinker. Journal of Polymer Science Part A-Polymer Chemistry 38(2000): 2804-2814.
38. Wang, X.P.; and Shen, Z.Q. Studies on the effects of copper salts on the separation performance of chitosan membranes. Polymer International 49(2000): 1426-1433.
39. Yeom, C.K.; Kim, C.U.; Kim, B.S.; Kim, KJ; and Lee, J.M. Recovery of anionic surfactant by RO process. Part I. Preparation of polyelectrolyte-complex anionic membrane. Journal of Membrane Science 143(1998): 207-218.
40. Zeng, X.; and Ruckenstein, E. Cross-linked macroporous chitosan anion-exchange membranes for protein separations. Journal of Membrane Science 148(1998): 195-205.

41. Qunhui, G.; Ohya, H.; and Negishi, Y. Investigation of the permselectivity of chitosan membrane used in pervaporation separation II. Influences of temperature and membrane thickness. Journal of Membrane Science 98(1995): 223-232.
42. Fang, Y.E.; Cheng, Q.; and Lu, X.B. Kinetics of in vitro drug release from chitosan/gelatin hybrid membranes. Journal of Applied Polymer Science 68(1998): 1751-1758.
43. Cardinal, J.R., Curatolo, W.J., and Ebert, C.D. U.S. Patent No. 4,895,724 (1990).
44. Yi, X.; Portnoy, J.; and Pellegrino, J. Diffusion measurements using ATR-FTIR spectroscopy: Acetone diffusion in polypropylene-use of pentrant fluid pressure to improve sample/IRE contact. Journal of Polymer Science: Part B: Polymer Physics 38(2000): 1773-1787.
45. Muller, G.; and Riedel, C. Quantitative comparison of ATR-IR spectra of LB and bulk layers of 22-tricosenic acid on inorganic supports. Fresenius Journal of Analytical Chemistry 365(1999): 43-47.
46. Buffeteau, T.; Desbat, B.; and Eyquem, D. Attenuated total reflection Fourier transform infrared microspectroscopy: Theory and application to polymer samples. Vibrational Spectroscopy 11(1996): 29-36.
47. Padermshoke A. Surface characterization of polycarbonate by ATR FT-IR Spectroscopy. Master's Thesis, Program of Petrochemistry and Polymer Science, Faculty of Science, Chulalongkorn University, 1999.
48. Ohta, K.; and Iwamoto, R. Applied Spectroscopy 39(1985): 418- .
49. Hansen, W.N. Spectrochim Acta 21(1965): 815- .
50. Mirabella, F.M. Spectroscopy 5(1990): 20- .
51. Urban, M.W. Attenuated total reflectance spectroscopy of polymer: theory and practice. District of Columbia: American Chemical Society, 1996.
52. Fujiyama, T.; Herrin, J.; and Crawford, B.L. Applied Spectroscopy 24(1970).



APPENDICES

สถาบันวิทยบริการ
จุฬาลงกรณ์มหาวิทยาลัย

Appendix A

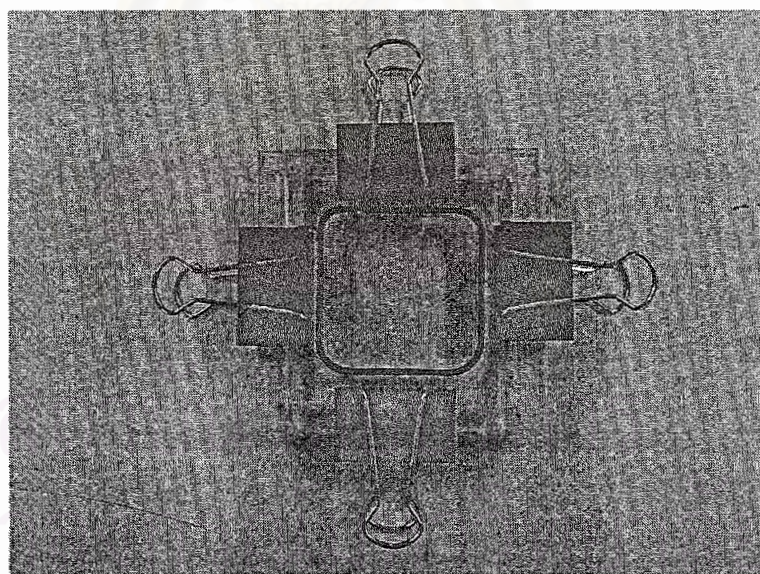
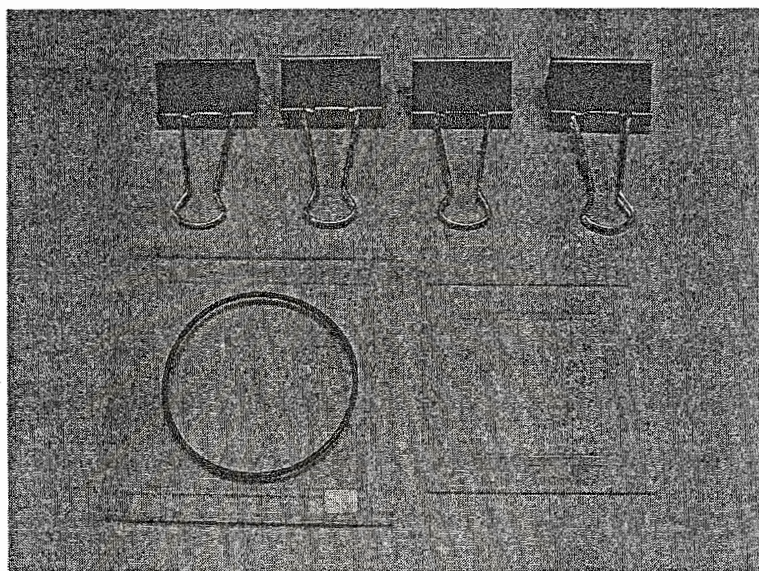
Pictures of accessories used in this research



Bruker Vector 33 FT-IR Spectrometer



Variable angle single attenuated total reflection accessories from Harrick (Seagull™)



Mold and accessories used for one-side crosslinking

Appendix B

Programs used for nk values calculation.

Nk_cal_main

```

%This program use to calculate nk value.

clear;
%function [n,k]=Equation_nk_Gen(wnj)
%global PEAK_POSITION K_MAX HWHH N_INFINITY
global Y A_bulk t0 MSEVF Dp wn
%Import data from nk_cal.data and subprogram
nk_cal_data;
Read_Intensity_main_for_nk_cal;
disp('Y = ');
disp(Y);
A_bulk = Y;
disp('A_bulk = ');
disp(A_bulk);
t0_gen_matrix;
wn_gen_matrix;
MSEVF_gen_matrix;
%disp(MSEVF)
%pause;
dp_gen_matrix;
%Y = the selected wavenumber from program "Read_Intensity_main"
%in metrix form, m*n = number of spectra(file_in)* number of
%calculated wavenumber(wn_cal)
%pause;
disp('t0='); disp(t0);
disp('Dp='); disp(Dp);
disp('MSEVF=');disp(MSEVF);
disp('wn='); disp(wn);
%calculation
nk = A_bulk.*cos(t0)*n0*log(10)./[2*pi*wn.*MSEVF.*Dp];
disp('nk = ');
disp(nk);
%pause;
plot(t0_in(1,:),nk(:,1),'rd-',t0_in(1,:),nk(:,2),'b+-')
disp('finish');

```

Nk_cal_data

```

%This program use to calculate nk value.

clear;
%file_out = char('nk_cal. ');
global Y A_bulk t0 MSEVF Dp wn

%wn_cal = the wavenumbers u want to calculate nk value
wn_cal = [1640 1560];%for chitosan
%wn_cal = [2920 1458 1376];%for nujol

%file_in are series of ASCII files u want to import spectral
%intensity (at various wavenumbers)
%Remark : All input spectral must be in ASCII format with the same
%resolution. The file name of all spectra must have the
%same length (including name and extension).

file_in = char('2P_37deg_cts_n1o4_k02.Abs',...
              '2P_39deg_cts_n1o4_k02.Abs',...
              '2P_41deg_cts_n1o4_k02.Abs',...
              '2P_43deg_cts_n1o4_k02.Abs',...
              '2P_45deg_cts_n1o4_k02.Abs',...
              '2P_47deg_cts_n1o4_k02.Abs',...
              '2P_49deg_cts_n1o4_k02.Abs');

%n0 is refractive index of Ire
n0 = 4.0;
%nf id refractive index of film
nf = 1.5;
%t0 is matrix[1,:]which each element is angle of incidence of each
%ASCII file in "file_in".So member of files in "file_in" must equal
%to the elements of matrix "t0".
t0_in = [37 39 41 43 45 47 49];

```

สถาบันวิทยบริการ
จุฬาลงกรณ์มหาวิทยาลัย

Read_Intensity_main_for_nk_cal

```

%This program is for reading/importing spectral intensity
%at various wavenumbers from multiple ASCII file.
%All input spectral must be in ASCII format with the same
%resolution. The file name of all spectra must have the
%same length (including name and extension).

global Y A_bulk t0 MSEVF Dp
nk_cal_data;
%Read_Intensity_data;
%Load Spectrum
temp=load(file_in(1,:));
xi= temp(:,1);
%disp(xi);
%pause;
%test frequency
del_x = round(((xi(size(xi,1),1)-xi(1,1))/(size(xi,1)-1))*1000)/1000;
%disp(del_x);
%pause;
j_x = [];
%disp(j_x);
%pause;

for j = 1:size(wn_cal,2)
    %j_x = the position of selected wavenumber
    %begin from 1 at wn4000 to 1868 at wn400
    j_x = [j_x find(abs(xi-wn_cal(j))<abs(del_x/2))];
end
Y = [];
for i = 1:size(file_in,1)%set running loop to equal the size of
    %first column of file_in
    temp=load(file_in(i,:));
    x = temp(:,1); y = temp(:,2);
    resolution_compatibility(x,xi);

    Y = [Y; y(j_x)'];
end
%disp('Y =');
%disp(Y);

%Exporting the Output
%Writing to ASCII Files
%disp('START WRITING ASCII FILES');
disp('finish');
    %file_name=file_out; %export Reflectance
    %data_out=[wn_cal;Y];
    %size(data_out);
    %dlmwrite(file_name,data_out,'\t');
%disp('FINISH WRITING ASCII FILES');

```

t0_gen_matrix

*%This program is used to generate t0
%in matrix form.*

```
global Y A_bulk t0 MSEVF Dp wn
```

```
%input data  
nk_cal_data;  
for i=1:size(t0_in,2)  
    for j=1:size(wn_cal,2)  
        t0_deg(i,j)=t0_in(i);  
    end  
end  
disp('t0_deg=');  
disp(t0_deg);  
t0=t0_deg*pi/180;  
disp('t0=');  
disp(t0);  
disp('finish');  
cos(t0*pi/180);
```

wn_gen_matrix

*%This program is used to generate wn
%in matrix form.*

```
%input data  
global Y A_bulk t0 MSEVF Dp wn  
nk_cal_data;  
for i=1:size(t0_in,2)  
    for j=1:size(wn_cal,2)  
        wn(i,j)=wn_cal(j)/10000;  
    end  
end  
disp('wn=');  
disp(wn);  
%disp('finish');
```

สถาบันวิทยบริการ
จุฬาลงกรณ์มหาวิทยาลัย

MSEVF_gen_matrix

```

%This program is used to generate MSEVF
%in matrix form.

global Y A_bulk t0 MSEVF Dp wn
%input data
nk_cal_data;
for i=1:size(t0_in,2)
    for j=1:size(wn_cal,2)
        nf0=nf/n0;
        Ex(i,j)=4*cos(t0(i,j))^2*(sin(t0(i,j))^2-nf0^2)/((1-
nf0^2)*((1+nf0^2)*(sin(t0(i,j)))^2-nf0^2));

        Ey(i,j)=(2*n0*cos(t0(i,j)))^2/(n0^2-nf^2);

        Ez(i,j)=4*cos(t0(i,j))^2*sin(t0(i,j))^2/((1-
nf0^2)*((1+nf0^2)*(sin(t0(i,j)))^2-nf0^2));
        %formula from Dr.sanong 's thesis page 78 eq. 12,13,14

        %MSEVF(i,j)=Ex(i,j)+Ez(i,j);%for p polarization
        %MSEVF(i,j)=Ey(i,j);%for s polarization
        MSEVF(i,j)=[Ex(i,j)+Ey(i,j)+Ez(i,j)]/2;%for n polarization

        %disp('run');
    end
end
disp('MSEVF=');
disp(MSEVF);

```

Dp_gen_matrix

```

%This program is used to generate Penetration Depth
%of p-polarization in matrix form

%input data
global Y A_bulk t0 MSEVF Dp
nk_cal_data;
for i=1:size(t0_in,2)
    for j=1:size(wn_cal,2)
        Dp(i,j)=1./(2*pi*(wn(i,j))*n0.*sqrt(sin(t0(i,j))^2-
nf.^2/n0^2));
    end
end
disp('Dp=');
disp(Dp);

```

Appendix C

Data of nk values calculation

Simulated spectra k=0.02

Angle of incidence	Spectral intensity		nk values	
	1654 cm ⁻¹	1564 cm ⁻¹	1654 cm ⁻¹	1564 cm ⁻¹
37	0.0089	0.0090	0.0264	0.0266
39	0.0080	0.0081	0.0267	0.0268
41	0.0073	0.0073	0.0268	0.0270
43	0.0066	0.0067	0.0270	0.0271
45	0.0061	0.0061	0.0271	0.0272
47	0.0056	0.0056	0.0272	0.0273
49	0.0051	0.0051	0.0272	0.0274

Simulated spectra k=0.5

Angle of incidence	Spectral intensity		nk values	
	1654 cm ⁻¹	1564 cm ⁻¹	1654 cm ⁻¹	1564 cm ⁻¹
37	0.2074	0.2401	0.6158	0.7128
39	0.1892	0.2178	0.6294	0.7248
41	0.1732	0.1986	0.6400	0.7338
43	0.1591	0.1817	0.6484	0.7407
45	0.1465	0.1668	0.6553	0.7462
47	0.1351	0.1534	0.6609	0.7506
49	0.1247	0.1413	0.6656	0.7542

nujol

Angle of incidence	Spectral intensity		nk values	
	1460 cm^{-1}	1376 cm^{-1}	1460 cm^{-1}	1376 cm^{-1}
37	0.0428	0.0221	0.1271	0.0656
39	0.0368	0.0184	0.1224	0.0622
41	0.0330	0.0169	0.1219	0.0624
43	0.0299	0.0152	0.1219	0.0620
45	0.0274	0.0140	0.1226	0.0626
47	0.0250	0.0128	0.1223	0.0626
49	0.0233	0.0119	0.1243	0.0635

Uncrosslinked chitosan film, mold-side

Angle of incidence	Spectral intensity		nk values	
	1654 cm^{-1}	1564 cm^{-1}	1654 cm^{-1}	1564 cm^{-1}
37	0.0098	0.0491	0.0291	0.1458
39	0.0083	0.0426	0.0276	0.1417
41	0.0074	0.0382	0.0273	0.1411
43	0.0066	0.0349	0.0269	0.1422
45	0.0062	0.0315	0.0277	0.1409
47	0.0058	0.0288	0.0284	0.1409
49	0.0051	0.0268	0.0272	0.1430

Uncrosslinked chitosan film, air-side

Angle of incidence	Spectral intensity		nk values	
	1654 cm ⁻¹	1564 cm ⁻¹	1654 cm ⁻¹	1564 cm ⁻¹
37	0.0117	0.0597	0.0347	0.1773
39	0.0090	0.0499	0.0299	0.1660
41	0.0075	0.0430	0.0277	0.1589
43	0.0063	0.0373	0.0257	0.1520
45	0.0058	0.0340	0.0259	0.1521
47	0.0053	0.0314	0.0259	0.1536
49	0.0048	0.0290	0.0256	0.1548

10 minutes crosslinked chitosan film, mlod-side

Angle of incidence	Spectral intensity		nk values	
	1654 cm ⁻¹	1564 cm ⁻¹	1654 cm ⁻¹	1564 cm ⁻¹
37	0.0116	0.0567	0.0344	0.1684
39	0.0098	0.0496	0.0326	0.1650
41	0.0088	0.0444	0.0325	0.1641
43	0.0078	0.0401	0.0318	0.1634
45	0.0072	0.0367	0.0322	0.1642
47	0.0068	0.0337	0.0333	0.1649
49	0.0061	0.0313	0.0326	0.1670

สถาบันวิทยบริการ
จุฬาลงกรณ์มหาวิทยาลัย

10 minutes crosslinked chitosan film, air-side

Angle of incidence	Spectral intensity		nk values	
	1654 cm^{-1}	1564 cm^{-1}	1654 cm^{-1}	1564 cm^{-1}
37	0.0178	0.0569	0.0529	0.1689
39	0.0145	0.0458	0.0482	0.1524
41	0.0126	0.0395	0.0466	0.1460
43	0.0115	0.0359	0.0469	0.1463
45	0.0106	0.0330	0.0474	0.1476
47	0.0100	0.0308	0.0489	0.1507
49	0.0093	0.0285	0.0496	0.1521

100 minutes crosslinked chitosan film, mold-side

Angle of incidence	Spectral intensity		nk values	
	1654 cm^{-1}	1564 cm^{-1}	1654 cm^{-1}	1564 cm^{-1}
37	0.0184	0.0666	0.0546	0.1977
39	0.0147	0.0570	0.0489	0.1897
41	0.0135	0.0513	0.0499	0.1896
43	0.0122	0.0465	0.0497	0.1895
45	0.0111	0.0423	0.0497	0.1892
47	0.0104	0.0393	0.0509	0.1923
49	0.0095	0.0364	0.0507	0.1942

สถาบันวิทยบริการ
จุฬาลงกรณ์มหาวิทยาลัย

100 minutes crosslinked chitosan film, air-side

Angle of incidence	Spectral intensity		nk values	
	1654 cm ⁻¹	1564 cm ⁻¹	1654 cm ⁻¹	1564 cm ⁻¹
37	0.0157	0.0409	0.0466	0.1214
39	0.0135	0.0350	0.0449	0.1165
41	0.0121	0.0312	0.0447	0.1153
43	0.0108	0.0278	0.0440	0.1133
45	0.0097	0.0252	0.0434	0.1127
47	0.0093	0.0203	0.0455	0.1125
49	0.0085	0.0214	0.0454	0.1142

1000 minutes crosslinked chitosan film, mold-side

Angle of incidence	Spectral intensity		nk values	
	1654 cm ⁻¹	1564 cm ⁻¹	1654 cm ⁻¹	1564 cm ⁻¹
37	0.0185	0.0549	0.0549	0.1630
39	0.0159	0.0479	0.0529	0.1594
41	0.0144	0.0423	0.0532	0.1563
43	0.0125	0.0379	0.0509	0.1545
45	0.0118	0.0348	0.0528	0.1557
47	0.0105	0.0318	0.0514	0.1556
49	0.0100	0.0294	0.0534	0.1569

สถาบันวิทยบริการ
จุฬาลงกรณ์มหาวิทยาลัย

1000 minutes crosslinked chitosan film, air-side

Angle of incidence	Spectral intensity		nk values	
	1654 cm^{-1}	1564 cm^{-1}	1654 cm^{-1}	1564 cm^{-1}
37	0.0125	0.0359	0.0371	0.1066
39	0.0099	0.0295	0.0329	0.0982
41	0.0089	0.0255	0.0329	0.0942
43	0.0076	0.0225	0.0310	0.0917
45	0.0070	0.0199	0.0313	0.0890
47	0.0063	0.0181	0.0308	0.0885
49	0.0059	0.0164	0.0315	0.0875



สถาบันวิทยบริการ
จุฬาลงกรณ์มหาวิทยาลัย

VITAE

Mr. Vuthipong Puengpipat was born in Ratchaburi, Thailand, on September 23, 1976. He received the second class honours in Bachelor of Science degree majoring in Polymer Science and Textile from the Department of Materials Science, Chulalongkorn University in 1998. He started as a graduate student with a major in Applied Polymer Science and Textile Technology, Chulalongkorn University in June 1998 and completed the program in September 2001.



สถาบันวิทยบริการ
จุฬาลงกรณ์มหาวิทยาลัย